Feature Review

CellPress

FDA-approved small-molecule kinase inhibitors

Peng Wu[1], Thomas E. Nielsen[2], and Mads H. Clausen[1,3]

[1] Department of Chemistry, Technical University of Denmark, DK-2800 Kgs. Lyngby, Denmark
[2] Protein and Peptide Chemistry, Novo Nordisk A/S, DK-2760 Måløv, Denmark
[3] Center for Nanomedicine and Theranostics, Technical University of Denmark, DK-2800 Kgs. Lyngby, Denmark

Kinases have emerged as one of the most intensively pursued targets in current pharmacological research, especially for cancer, due to their critical roles in cellular signaling. To date, the US FDA has approved 28 small-molecule kinase inhibitors, half of which were approved in the past 3 years. While the clinical data of these approved molecules are widely presented and structure–activity relationship (SAR) has been reported for individual molecules, an updated review that analyzes all approved molecules and summarizes current achievements and trends in the field has yet to be found. Here we present all approved small-molecule kinase inhibitors with an emphasis on binding mechanism and structural features, summarize current challenges, and discuss future directions in this field.

Kinase inhibitors: a burgeoning field

The past one and a half decades witnessed an unparalleled success in the development of therapeutically useful kinase inhibitors, powered by tremendous progress in both academic and industrial settings. The milestone approval of the first kinase inhibitor, imatinib, in 2001 by the FDA, was followed by a slow yet steady approval of kinase inhibitors in the first 10 years of this century with almost one new approval per year on average. Concurrently, our understanding of kinase signaling networks and disease pathology steadily grew, culminating in the approval of 15 new small-molecule kinase inhibitors from January 2012 to February 2015 – an unparalleled achievement in the history of pharmaceutical research. By April 2015, a total of 28 small-molecule kinase inhibitors have been approved (see the supplementary material online), along with a large number of other compounds currently being evaluated in clinical and preclinical trials. In addition, more than 1 million publications on kinases have been released, more than 5000 crystal structures of kinases with or without small molecules have been solved, inhibition assays have been developed for more than four-fifths of the human kinome, and small-molecule kinase inhibitors have been identified for about one-fifth of the human kinome. All of these facts reflect the surging interest in this field. Thus, it is now safe to state that the development of small-molecule kinase inhibitors has emerged as one of the most extensively pursued areas of drug discovery. Despite the abundance of data, common binding modes and structural features of approved small-molecule kinase inhibitors are rarely reported in a systematic way that is easily accessible. Instead, information on individual inhibitors and their analogs appears scattered and fragmented. In this review, we provide a comprehensive overview and discuss the mechanisms of function and structural binding features of approved small-molecule kinase inhibitors based on co-crystal structures. With the notion that 15 kinase inhibitors were approved by the FDA in the short period from 2012 to February 2015, emphasis will be put on those small molecules for which few SAR discussions have been presented. The intention of this review is to compile structural and binding information useful for the discovery of new kinase inhibitors, summarize current limitations and challenges, and propose future directions in the field in light of the most successful design-to-approval examples.

Kinases

Kinases catalyze the transfer of the γ-phosphate group of ATP onto a substrate, mediate most signal transductions [1], and regulate various cellular activities, including proliferation, survival, apoptosis, metabolism, transcription, differentiation, and a wide array of other cellular processes [2]. Accumulating pharmacological and pathological evidence has revealed that kinases are promising drug targets for the treatment of numerous diseases [3] such as cancers [4–6], inflammatory diseases [7,8], central nervous system (CNS) disorders [9], cardiovascular diseases [10], and complications of diabetes [11].

Pioneering studies on the characterization of the phosphorylase kinase in the 1950s [12–14] and the identification of the first kinase signaling cascade involving protein kinase A (PKA) in 1968 [15] constituted the first few pieces of the jigsaw puzzle of kinase cascades. The 'decade of protein kinase cascades' in the 1990s witnessed the unfolding of the mitogen-activated protein kinases/extracellular signal-regulated kinase (MAPK/ERK) (also known as Ras–Raf–MEK–ERK) pathway, the Janus kinase (JAK) pathway, and the phosphoinositide 3-kinase (PI3K) pathway [16,17]. So far, 518 human kinases and more than 900 genes encoding proteins with kinase activity have been confirmed [18,19]. Albeit accounting for only about 5% of the total number of protein-coding genes [20], kinases

Corresponding author: Wu, P. (penwu@kemi.dtu.dk).
Keywords: cancer; protein kinase; lipid kinase; tyrosine kinase; serine/threonine kinase; crystal structure.

0165-6147/
 http://dx.doi.org/10.1016/j.tips.2015.04.005

comprise one of the largest classes of proteins encoded by the human genome.

Kinase inhibitors

Although diverse in primary amino acid sequence, the human kinases share a great degree of similarity in their 3D structures, especially in their catalytically active kinase domain where the ATP-binding pocket is located: a β sheet containing N-terminal lobe (N-lobe), an α helix-dominated C-terminal lobe (C-lobe), and a connecting hinge region [21]. ATP binds in the cleft formed between the N- and C-lobes and most kinase inhibitors perturb binding through interactions with this region. A flexible activation loop starting with a conserved amino acid sequence Asp-Phe-Gly (DFG) controls access to the active site [22] (Figure 1A). Categorized by binding modes, kinase inhibitors can be grouped into two classes: irreversible and reversible. The former tend to covalently bind with a reactive nucleophilic cysteine residue proximal to the ATP-binding site, resulting in the blockage of the ATP site and irreversible inhibition. The latter can be further classified into four main types based on the conformation of the binding pocket and the DFG motif [23,24] (Figure 1B). Type I inhibitors are ATP-competitive inhibitors that bind to the active forms of kinases with the aspartate residue of the DFG motif facing into the active site of the kinase. Type II inhibitors bind to the inactive forms of kinase with the aspartate residue of the DFG motif protruding outward from the ATP-binding site of the kinase. Many type II inhibitors exploit specific pockets accessible in a region adjacent to the ATP-binding site due to the rotation of the DFG motif. In the type III binding mode, inhibitors bind exclusively in an allosteric pocket adjacent to ATP without making any interaction with the ATP-binding pocket. Type IV inhibitors bind to an allosteric site remote from the ATP-binding pocket [25]. Some kinase inhibitors, such as bisubstrate and bivalent inhibitors (type V) [26], exhibit more than one of these binding modes.

Small-molecule kinase inhibitors are useful reagents to investigate and elucidate kinase functions in various

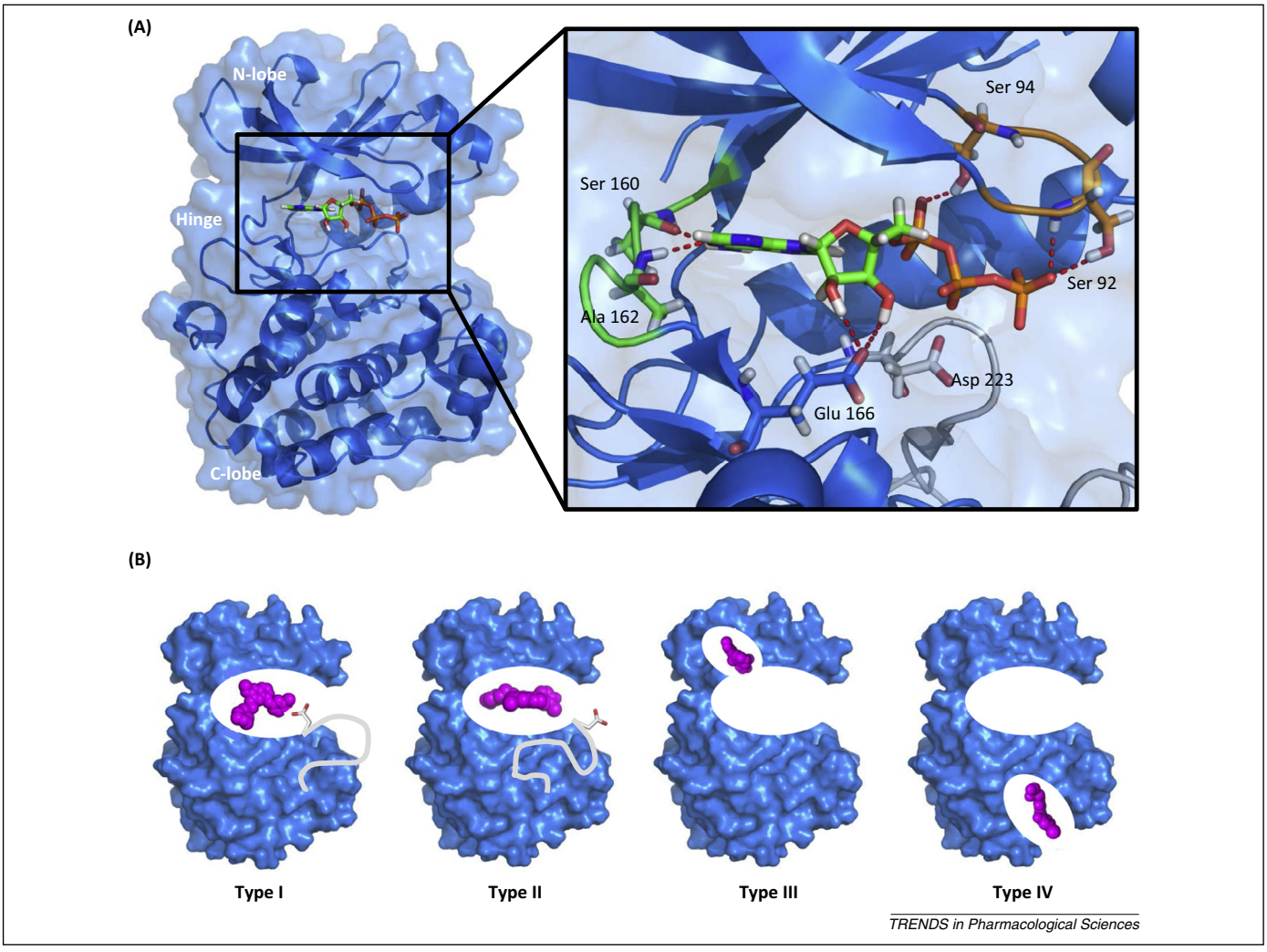

Figure 1. Kinase structure and different types of reversible small-molecule kinase inhibitor. **(A)** Co-crystal structure of PDK1 with ATP (adenine and ribose in green backbone, phosphate groups in orange) with the enlarged area showing the structural elements around the ATP-binding site. Hydrogen bonds in red broken lines; hinge region and hinge residues in green backbone; P-loop and P-loop residue in brown–orange backbone; the aspartate residue of the Asp-Phe-Gly (DFG) motif and the activation loop in white backbone [Protein Data Bank (PDB) ID: 4RRV, 1.41 Å]. **(B)** Four types of reversible binding mode. Type I inhibitors bind to the active conformation of the kinase with the aspartate residue (white backbone) of the DFG motif pointing into the ATP-binding pocket; type II inhibitors bind and stabilize the inactive conformation of the kinase with the flipped aspartate residue facing outward of the binding pocket; type III inhibitors occupy an allosteric pocket that is adjacent to the ATP-binding pocket but does not overlap with it; type IV inhibitors bind to an allosteric pocket remote from the ATP-binding pocket.

cellular activities [5]. The dominant dogma that the kinase domain was too conserved to enable selective inhibition by small molecules was challenged in the late 1980s when the first examples of selective kinase inhibitors against the epidermal growth factor receptor (EGFR) were reported [27,28]. Since then, a large number of kinase inhibitors of various structural features and inhibition profiles have been identified aided by the deepening understanding of structural biology [3], especially the kinase/inhibitor binding complex elucidated by high-resolution X-ray crystallography [29,30].

Among the 28 clinically approved kinase inhibitors, most are tyrosine kinase inhibitors [31], a few are serine/threonine kinase inhibitors, and one, idelalisib, is a lipid kinase inhibitor that was approved in July 2014 (Figure 2). Judged by different binding modes, 26 are reversible inhibitors and the remaining two, afatinib and ibrutinib, are irreversible inhibitors. Despite several promising allosteric kinase inhibitors being currently in clinical trials at different stages, trametinib is the only type III inhibitor approved so far. In this review, approved small-molecule kinase inhibitors are discussed and grouped into different classes based on their binding modes and targets.

Approved tyrosine kinase inhibitors

Reversible non-receptor tyrosine kinase (NRTK) inhibitors

BCR-Abl was the first kinase for which a small-molecule inhibitor was successfully approved [32]. On another note, being the first approved kinase inhibitor and a revolutionary success for the treatment of chronic myeloid leukemia (CML) [17], imatinib has been the subject of various SAR studies to guide the design of next-generation inhibitors and provide a deeper understanding of the inhibition mechanism. Considerable efforts seek to develop inhibitors based on structural features derived from imatinib and its binding mode with BCR-Abl [33,34]. Five BCR-Abl inhibitors have been approved so far: imatinib (Gleevec®, Novartis), dasatinib (Sprycel®, Bristol-Myers Squibb), nilotinib (Tasigna®, Novartis), bosutinib (Bosulif®, Wyeth), and ponatinib (Iclusig®, Ariad Pharmaceuticals).

Imatinib, nilotinib, and ponatinib bind with inactive BCR-Abl with the DFG motif adopting an 'out' conformation, utilizing three binding pockets (Figure 3). The pyridine–pyrimidine moiety of imatinib forms a conserved hydrogen bond with hinge residue Met318. The tolyl group occupies a hydrophobic pocket and the amino group of the tolylaminopyrimidine moiety forms a hydrogen bond with the gatekeeper residue Thr315. The terminal piperazinylphenyl group binds inside an allosteric pocket, formed due to the flipped conformation of the DFG motif, where the piperazinyl amine forms bidentate ionic interactions with His361 and Ile360. In addition, hydrogen bonds are formed between the amide connecting link and Glu286, Asp 381 [35] (Figure 3A,B). Despite high efficacy and limited toxicity compared with traditional chemotherapy drugs, point mutations in the kinase domain of BCR-Abl led to the development of drug resistance against imatinib [36,37]. Thus, nilotinib was developed as a second-line therapy for CML that is imatinib resistant due to point mutations in BCR-Abl, including E255V, M351T, and F486S. Nilotinib shares the same pyridine–pyrimidine–aminotolyl moiety with imatinib, the difference being the long-chain binding within the allosteric pocket. The imidazole–phenyl moiety and the attached trifluoromethyl group make it possible for nilotinib to bind deeper and tighter within the allosteric pocket (Figure 3C,D). Nilotinib is potent against most mutations but not the common gatekeeper mutation T315I, which blocks the binding into the allosteric pocket due to mutation of the small threonine residue to a bulky isoleucine residue. In this context, ponatinib was developed as a new BCR-Abl inhibitor that exhibits potent T315I inhibitory activity. Instead of having a pyrimidineamino linker interacting with the gatekeeper residue Thr315, a slim alkyne linker that overcomes steric hindrance due to mutation of the gatekeeper residue was incorporated in ponatinib. Furthermore, ponatinib bears the piperizinylphenyl group of imatinib and the trifluoromethyl group of nilotinib, resulting in a more compact interaction with the allosteric pocket (Figure 3E,F).

Dasatinib and bosutinib are the two approved inhibitors that bind with the active conformation of BCR-Abl with the activation loop fully extended for substrate binding. As for dasatinib (Figure 4A), the nitrogen of the thiazole core and the attached amino group form hydrogen bonds with hinge residue Met318. The long hydroxyethylpiperazinyl tail is exposed to the solvent region. The terminal toluidine group points toward a hydrophobic pocket close to the gatekeeper residue Thr315, which

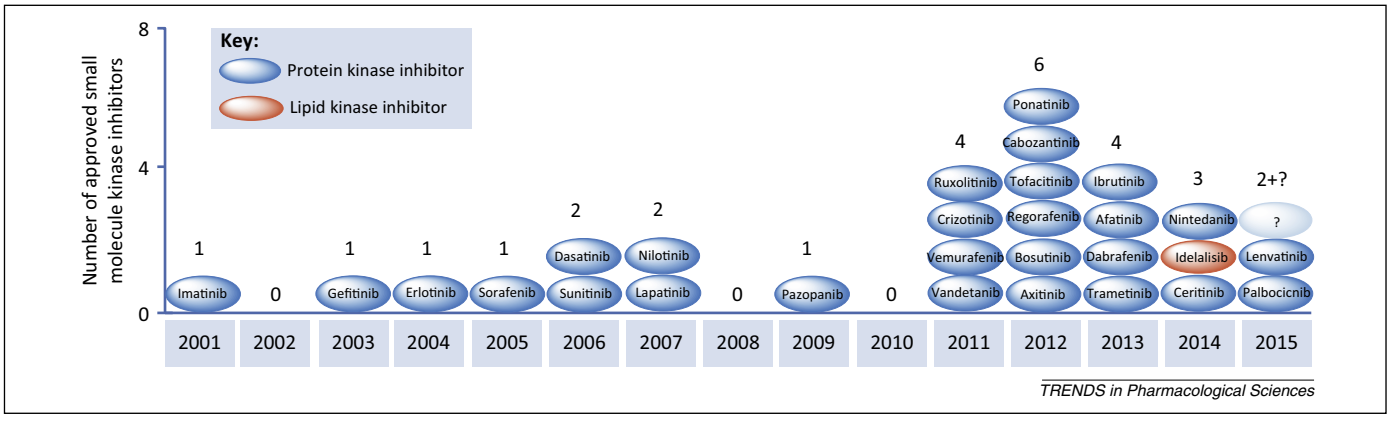

Figure 2. FDA-approved small-molecule kinase inhibitors (at April 2015).

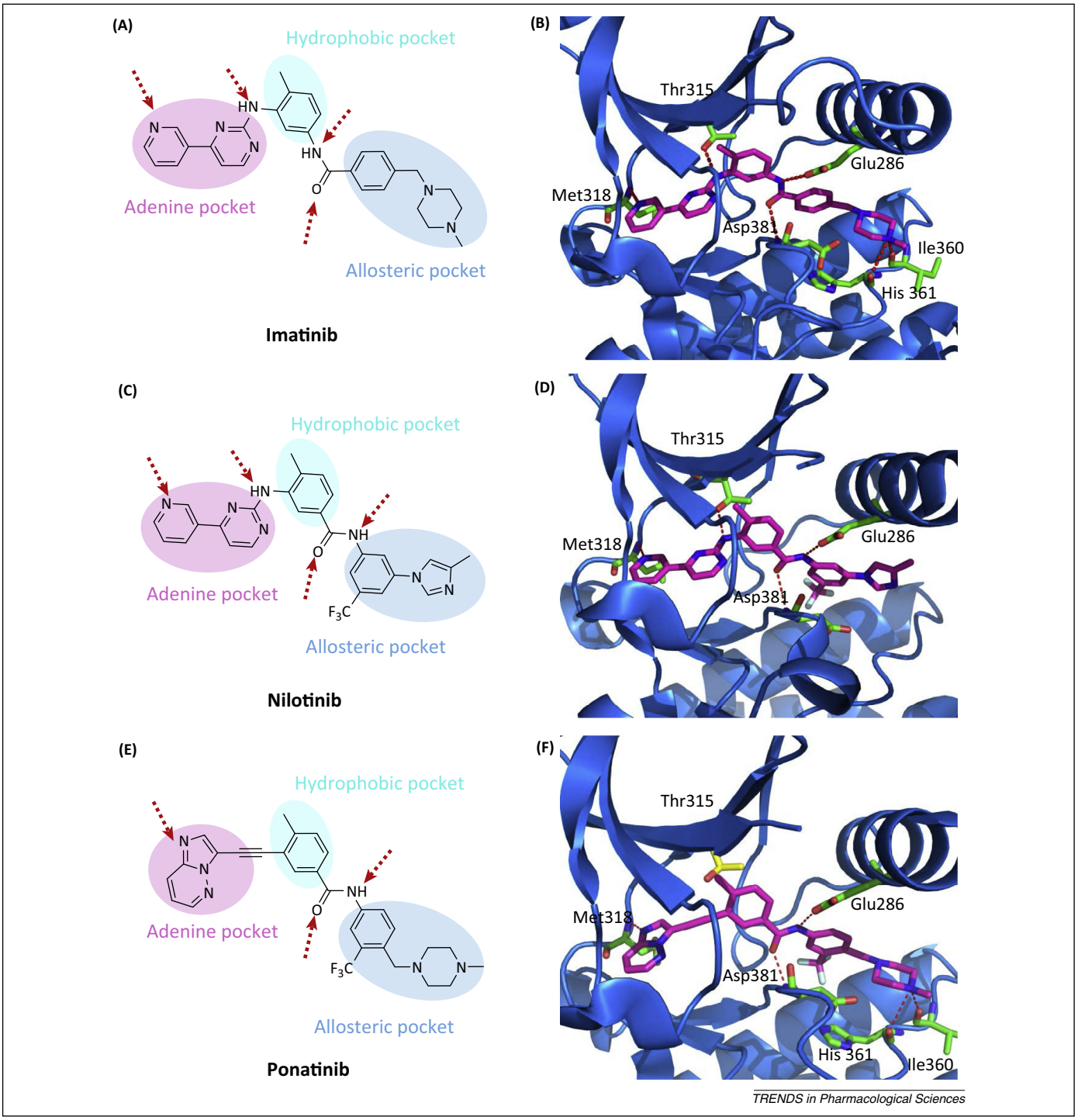

Figure 3. Type II inhibitors of BCR-Abl. **(A)** Chemical structure of imatinib and its depicted binding mode with BCR-Abl. **(B)** Imatinib co-crystal structure [Protein Data Bank (PDB) ID: 1IEP, 2.10 Å]. **(C)** Chemical structure of nilotinib and its depicted binding mode with BCR-Abl. **(D)** Nilotinib co-crystal structure (PDB ID: 3CS9, 2.21 Å). **(E)** Chemical structure of ponatinib and its depicted binding mode with BCR-Abl. **(F)** Ponatinib co-crystal structure with wild type BCR-Abl (PDB ID: 3OXZ, 2.20 Å). Small-molecule inhibitors are shown in magenta backbone, hydrogen bonds are indicated by red broken lines, and residues that interact with inhibitors through hydrogen bonds are shown in green backbone; π interactions formed between certain aromatic rings of these molecules and residues including Phe and Tyr are not illustrated in these ribbon-show figures. Co-crystal structures of ponatinib (PDB ID: 3IK3, 1.9 Å) and its analog (PDB ID: 3OY3, 1.95 Å) with mutant T315I [shown in yellow backbone in (F)] BCR-Abl have also been released.

interacts with the connecting amide link through a hydrogen bond (Figure 4B,C). Thus, T315I mutation-related drug resistance also occurs in patients treated with dasatinib. In contrast to the other four approved BCR-Abl molecules, bosutinib bears an anilinequinoline core that is similar to the anilinequinazoline core of some EGFR inhibitors (Figure 4D). A hinge hydrogen bond is formed between the quinoline nitrogen and the backbone amide of Met 318. The substituted aniline group occupies the hydrophobic pocket adjacent to Thr315. The nitrile group extends into another Thr315-adjacent pocket, which may host water molecules to form conserved water-mediated hydrogen bond interactions with small-molecule inhibitors to contribute to kinase selectivity [38]. Due to the

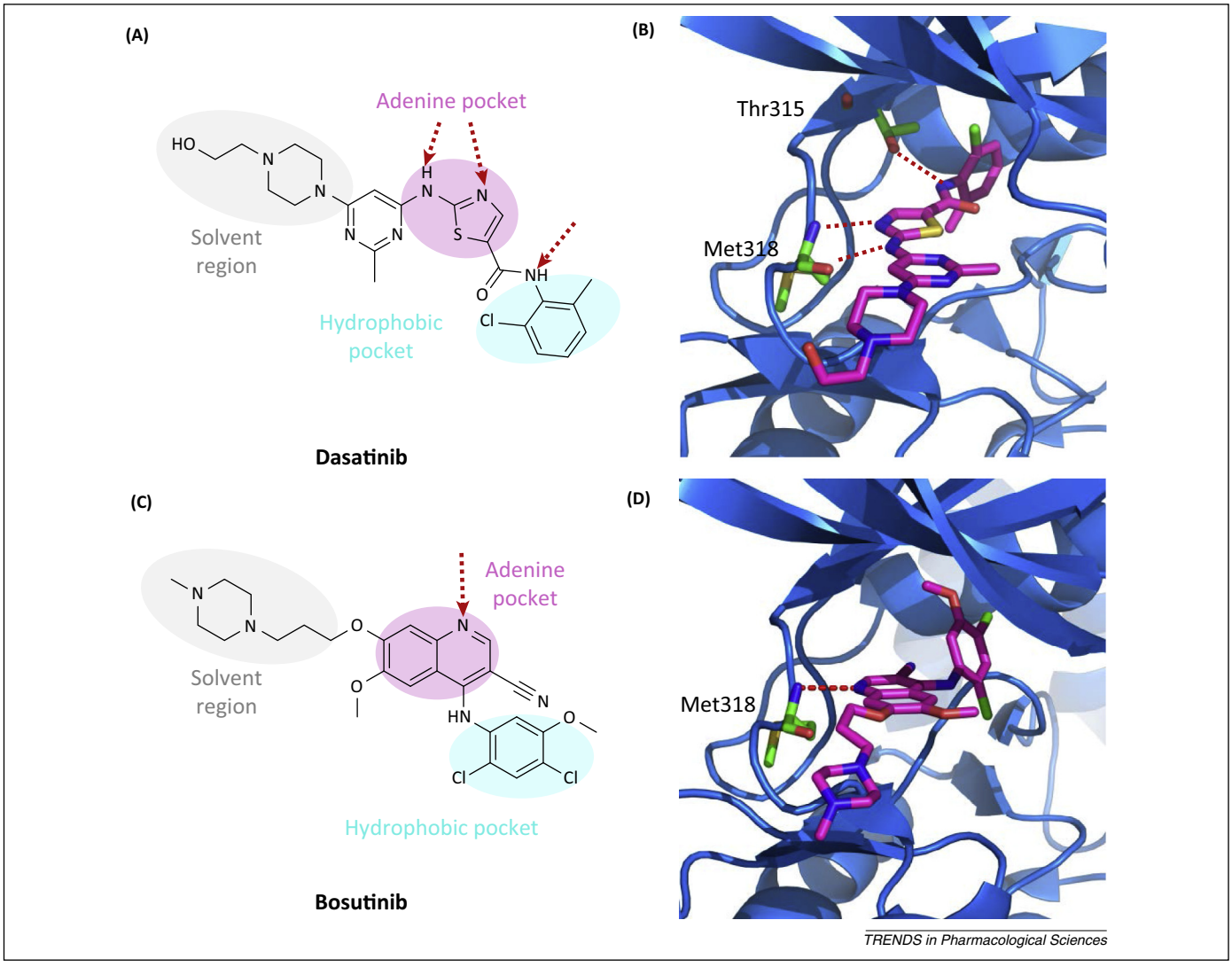

Figure 4. Inhibitors binding with active BCR-Abl. **(A)** Chemical structure of dasatinib and its depicted binding mode with BCR-Abl. **(B)** Dasatinib co-crystal structure [Protein Data Bank (PDB) ID: 2GQG, 2.40 Å]. **(C)** Surface show of the dasatinib-Abl co-crystal structure (PDB ID: 2GQG, 2.40 Å). **(D)** Chemical structure of bosutinib and its depicted binding mode with BCR-Abl. **(E)** Bosutinib co-crystal structure (PDB ID: 3UE4, 2.42 Å). **(F)** Surface show of the bosutinib–Abl co-crystal structure (PDB ID: 2GQG, 2.40 Å). Small-molecule inhibitors are shown in magenta backbone, hydrogen bonds are indicated by red broken lines, residues that interact with inhibitors through hydrogen bonds are shown in green backbone, the gatekeeper residue is shown in yellow backbone, and residues of the Asp-Phe-Gly (DFG) motif are shown in white backbone.

propensity of BCR-Abl to adopt a certain conformation at the low pH values needed for crystallization, the DFG motif of the bosutinib–Abl complex exhibits a conformation different from that of the dasatinib–Abl complex (Figure 4E,F). A bosutinib–Src complex with the DFG motif adopting the same conformation as shown in the dasatinib–Abl complex has been reported recently [38].

JAKs are a family of intracellular NRTKs that are required for multiple signaling pathways initiated by cytokines and growth factor receptors to phosphorylate signal transducer and activator of transcription (STAT) proteins [39,40]. Four isomers – JAK1, JAK2, JAK3, and tyrosine kinase 2 (TYK2) – have been identified as JAK family kinases. JAK3 is exclusively expressed in cells of the lymphoid lineage and plays important roles in the immune system [41], while the other three isoforms are ubiquitously expressed and regulate a range of physiological functions [42]. Although small-molecule kinase inhibitors against JAKs are potential agents for the treatment of autoimmune and neoplastic disorders [43], the development of isoform-selective JAK inhibitors is challenging due to the high sequence similarity among the four JAK kinases [7].

Ruxolitinib (Jakafi®, Incyte Corp.) was the first approved JAK inhibitor (Figure 5A). It inhibits both JAK1 and JAK2 and is used for the treatment of myeloproliferative disorders such as myelofibrosis. Tofacitinib (Xeljanz®, Pfizer) was approved by the FDA as a JAK3-selective inhibitor in 2012 for the treatment of rheumatoid arthritis (Figure 5B). However, the efficacy of tofacitinib has been hindered by side effects such as anemia and neutropenia, probably due to undesirable pan-JAK inhibition; thus, it was not approved by European regulatory agencies. Both molecules bear a pyrrolo[2,3-*d*]pyrimidine scaffold, and whereas no co-crystal structure of ruxolitinib with JAK has been published yet, crystal complexes of tofacitinib with JAK1, JAK2, and JAK3 are readily available [44,45]. Tofacitinib binds within the ATP pocket of JAKs.

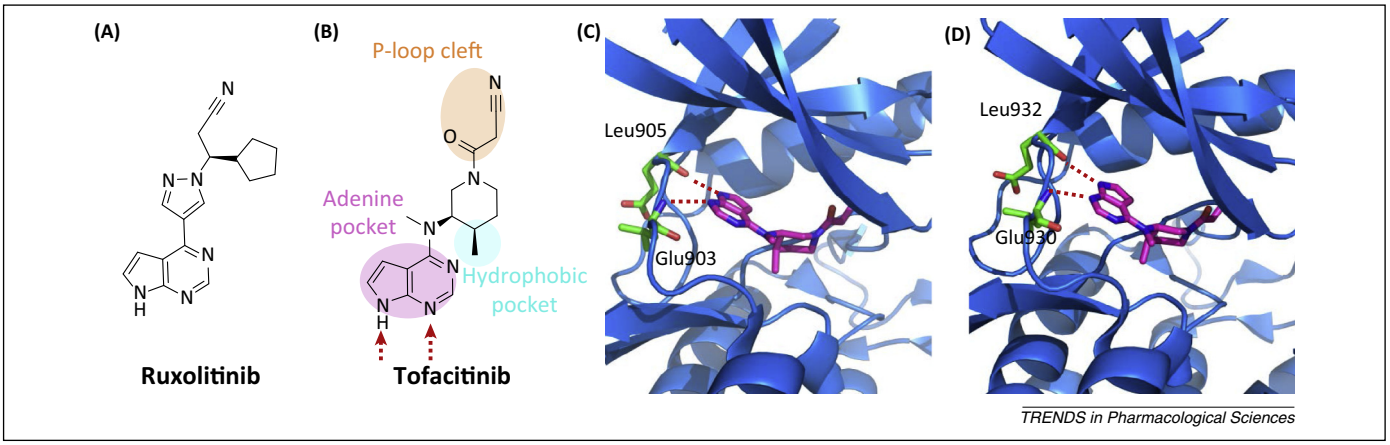

Figure 5. Janus kinase (JAK) inhibitors. **(A)** Chemical structure of ruxolitinib. **(B)** Chemical structure of tofacitinib and its depicted binding mode with JAK2/3. **(C)** Tofacitinib co-crystal structure with JAK3 [Protein Data Bank (PDB) ID: 3LXK, 2.0 Å]. **(D)** Tofacitinib co-crystal structure with JAK2 (PDB ID: 3FUP, 2.4 Å). Tofacitinib shown in magenta backbone, hydrogen bonds are indicated by red broken lines, and residues that interact with tofacitinib through hydrogen bonds are shown in green backbone.

The pyrrolo[2,3-*d*]pyrimidine scaffold forms two hydrogen bonds with hinge residues Leu905 and Glu903 in JAK3 (Leu932 and Glu930 in JAK2). The terminal cyanoacetyl handle extends into a cleft underneath the P-loop in the N-lobe. The methyl group of the piperidine ring occupies a small hydrophobic pocket in the C-lobe (Figure 5C,D). Compounds with better selectivity toward JAK3 and reduced side effects are currently being investigated as the next-generation JAK inhibitors [46,47].

Reversible receptor tyrosine kinase (RTK) inhibitors

ErbB, named for their homology to the erythroblastoma viral gene product *v-ErbB*, is a family of RTKs that includes four members: ErbB1/epidermal growth factor receptor (EGFR), ErbB2/human epidermal growth factor receptor 2 (Her2), ErbB3/Her3, and ErbB4/Her4 [48]. The ErbB cascade is one of the most extensively studied signaling transduction pathways [49,50] and the ErbB inhibitors gefitinib (Iressa®, AstraZeneca), erlotinib (Tarceva®, OSI Pharmaceuticals), lapatinib (Tykerb®, GlaxoSmithKline), vandetanib (Caprelsa®, AstraZeneca), and afatinib (Gilotrif®, Boehringer Ingelheim) constitute one of the largest groups of approved small-molecule kinase inhibitors. All five inhibitors bear a common quinazoline scaffold occupying the ATP adenine-binding pocket, a 4-amino substituent binding in a hydrophobic pocket close to the kinase hinge, and a long chain in the 6- and/or 7-position extending toward the solvent to increase the overall solubility of the molecule. In contrast to the other four reversible inhibitors, afatinib bears an enone moiety in the long solubilizing chain, enabling it to form a covalent bond. Thus, afatinib is discussed together with ibrutinib in the section on covalent inhibitors.

A complex of wild type EGFR with gefitinib was first reported in 2007 [51] (Figure 6A,B). Structures of EGFR kinases with mutations at L858R or T790M have also been solved by several different groups. Extensive efforts to crystallize drug-resistant double-mutant L858R+T790M EGFR failed to give diffraction-quality crystals until a structure of EGFR with L858R+T790M+V948R mutations was recently co-crystallized with gefitinib [52] (Figure 6C). In contrast to the wild type EGFR conformation that showed an active state with Leu858 buried in the kinase N-lobe, this mutant EGFR structure adopted an inactive-like state where the Arg858 residue is exposed to the solvent front. Although gefitinib, erlotinib, and vandetanib are the few inhibitors for which no experimental evidence regarding inactive state recognition has been collected so far, this gefitinib-mutant EGFR co-crystal structure showed that there may be no structural hindrance for these inhibitors to bind with the inactive form of EGFR. SAR and structural features obtained from these mutant kinase complexes provide a new dimension for the development of kinase inhibitors that may better address challenging issues regarding selectivity and drug resistance. Due to the high structural similarity, the erlotinib–EGFR complex showed the same binding mode as that of the gefitinib–EGFR complex, albeit with different 6,7-quinazoline substituents exposed in the solvent region [53] (Figure 6D–F).

Lapatinib is a dual EGFR and ErbB2 inhibitor. In contrast to the type I binding mode as shown for erlotinib and gefitinib, lapatinib binds with the inactive conformation of EGFR, utilizing not only the adenine pocket and the specific hydrophobic pocket but also an allosteric pocket formed due to the conformation change of the DFG motif [54] (Figure 6G,H). Equivalent to its binding with EGFR, lapatinib binds with the inactive conformation of ErbB4, which shares the same lapatinib-contacting residues with ErbB2 [55] (Figure 6I). Although it has been assumed that allosteric modulators like type II inhibitors may achieve higher selectivity compared with type I inhibitors due to the utilization of an allosteric pocket unfolded through the conformational change [56], some of the currently available allosteric inhibitors are highly nonselective and a recent binding mode analysis suggested that type II inhibitors do not show an intrinsic selectivity advantage over type I inhibitors [57].

Vandetanib is a multiple kinase inhibitor against EGFR, the vascular endothelial growth factor (VEGF) receptor (VEGFR), and RET [58]. Despite the absence of a vandetanib–EGFR complex, a co-crystal structure of vandetanib with RET of class XIV RTK showed the same type I binding as seen in gefitinib and erlotinib [58] (Figure 6J–L).

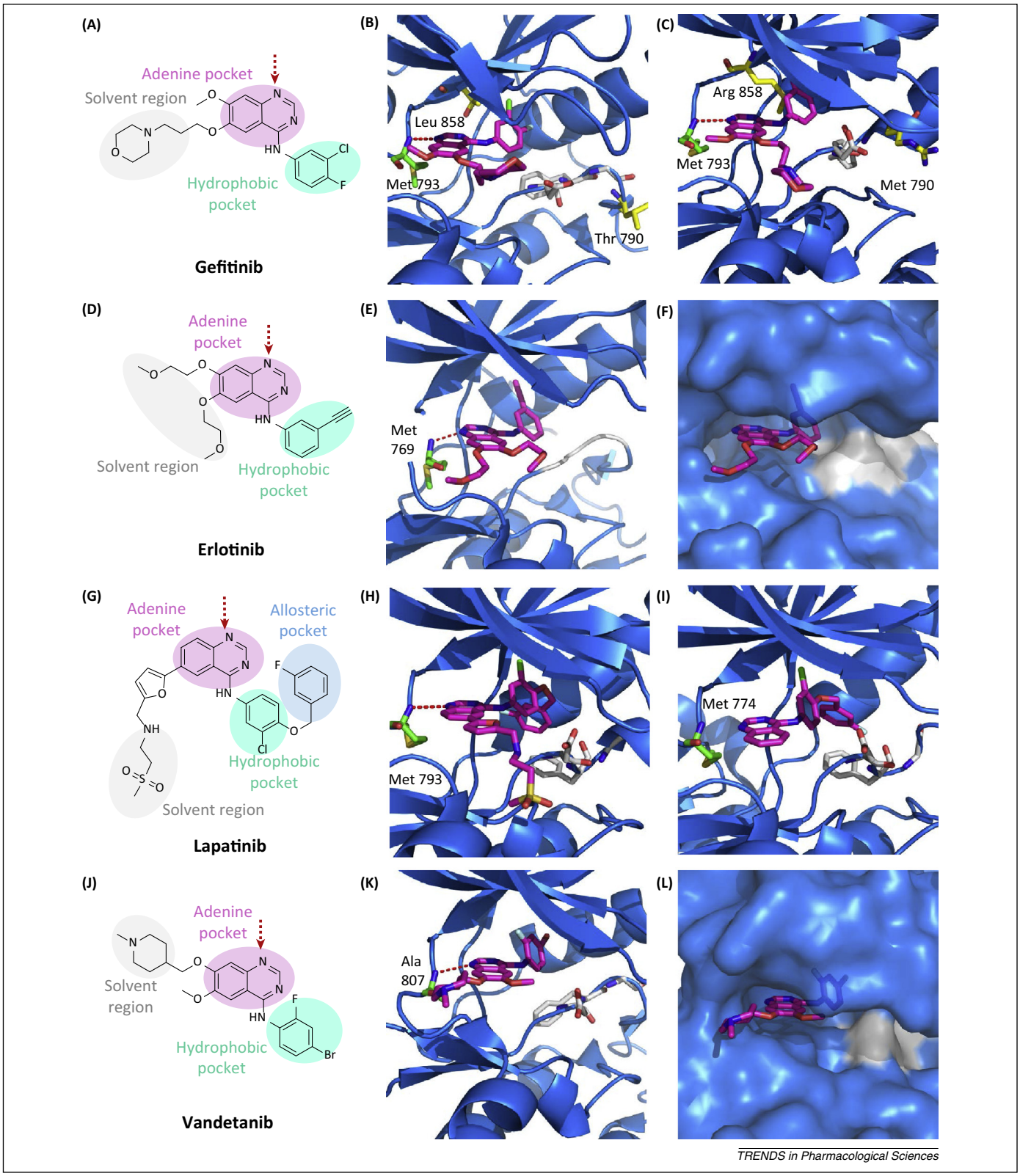

Figure 6. Small-molecule kinase inhibitors against ErbBs. **(A)** Chemical structure of gefitinib and its depicted binding mode with the epidermal growth factor receptor (EGFR). **(B)** Gefitinib co-crystal structure with wild type EGFR [Protein Data Bank (PDB) ID: 2ITY, 3.42 Å]. **(C)** Gefitinib co-crystal structure with mutant L858R+T790M+V948R EGFR (PDB ID: 4I22, 1.71 Å). **(D)** Chemical structure of erlotinib and its depicted binding mode with EGFR. **(E)** Erlotinib co-crystal structure with EGFR (PDB ID: 1M17, 2.60 Å). **(F)** Surface show of erlotinib co-crystal structure with EGFR (PDB ID: 1M17, 2.60 Å). **(G)** Chemical structure of lapatinib and its depicted binding mode with EGFR. **(H)** Lapatinib co-crystal structure with EGFR (PDB ID: 1XKK, 2.40 Å). **(I)** Lapatinib–ErbB4 complex, the methylsulfonylethanylaminomethylfuranyl moiety is not shown in this crystal structure (PDB ID: 3BBT, 2.80 Å). **(J)** Chemical structure of vandetanib and its depicted binding mode with RET. **(K)** Vandetanib co-crystal structure with RET (PDB ID: 2IVU, 2.50 Å). **(L)** Surface show of vandetanib co-crystal structure with RET (PDB ID: 2IVU, 2.50 Å). Small-molecule inhibitors are shown in magenta backbone, hydrogen bonds are indicated by red broken lines, residues that interact with inhibitors through hydrogen bonds are shown in green backbone, residue 858 and residue 790 in the gefitinib–EGFR complex are shown in yellow backbone, and residues of the Asp-Phe-Gly (DFG) motif are shown in white backbone.

VEGFRs, comprising three major isoforms (1, 2, and 3), are receptors of VEGF, which is an important signaling protein in vasculogenesis and angiogenesis [59,60]. Like Bcr-Abl and EGFR, VEGFR is among the earliest and most extensively studied kinases targeted by synthetic small molecules for cancer treatment. Seven approved small-molecule inhibitors target VEGFR as their primary target: sorafenib (Nexavar®, Bayer), sunitinib (Sutent®, Pfizer), pazopanib (Votrient®, GlaxoSmithKline), axitinib (Inlyta®, Pfizer), regorafenib (Stivarga®, Bayer), nintedanib (Ofev®, Boehringer Ingelheim), and lenvatinib (Lenvima®, Eisai Inc.).

The binding mode of VEGFR with small-molecule inhibitors has been the subject of SAR discussions in many studies due to the early resolution of corresponding co-crystal structures. General binding mode and common structural features are shown based on the VEGFR2 complexes that are available for four of the seven approved VEGFR inhibitors [61] (Figure 7A–H): the conserved hinge bond is formed between the picolinamide group of sorafenib with Cys919, the indolinone core of sunitinib with Glu917 and Cys919, the indazole core of axitinib with Glu917 and Cys919, and the indolinone core of nintedanib with Glu917 and Cys919. With the exception of sunitinib, the allosteric pocket formed due to the relocation of the DFG group is utilized by the remaining three molecules: the terminal 4-chloro-3-(trifluoromethyl)phenyl group of sorafenib binds in a deep hydrophobic allosteric pocket and the urea group lying in an allosteric channel forms hydrogen bonds with N-lobe residue Glu885 and the activation-loop residue Asp 1046; axitinib interacts with a small part of the allosteric pocket through its terminal benzamide group; and nintedanib binds with the allosteric pocket using its terminal methylcarboxy group. Another difference among these four compounds is the presence of a solubilizing chain: both sunitinib and nintedanib have a long terminal chain lying in the solvent region and axitinib's moderate-length pyridylvinyl chain extends to the solvent front, while sorafenib is buried inside the binding pocket without direct interaction with the solvent. In the case of nintedanib, ionic interactions are formed between the N-methylpiperazinyl group and Glu850. Regorafenib differs from sorafenib only by the presence of a fluorine atom (Figure 7I); thus, type II binding with VEGFR2 similar to that for sorafenib is expected. Both sorafenib and regorafenib are multitarget protein kinase inhibitors. Besides inhibition of VEGFR and B-raf, sorafenib has also been shown to be a potent low-nanomolar inhibitor of p38α through binding with its inactive conformation [Protein Data Bank (PDB) ID: 3GCS] [62]. A predicted type II binding mode of pazopanib with VEGFR2 is depicted (Figure 7J) based on a VEGFR2 complex with a similar indazolylpyrimidine-2,4-diamine compound that differs only in the aniline substituent at the 2-position of the pyrimidine-2,4-diamine [63]. Although a co-crystal structure of VEGFR2 with lenvatinib (PDB ID: 3WZD) was reported in November 2014 [64], for unspecified reasons it is still not accessible through the PDB database. It was reported that lenvatinib binds into both the ATP-binding site and a neighboring allosteric region of VEGFR2 with the DFG motif adopting an 'in' conformation (Figure 7K), making it an inhibitor that possesses both type I and II binding features [64].

Anaplastic lymphoma kinase (ALK) is a RTK that shares great sequence similarity with leukocyte tyrosine kinase (LTK) [65]. Chromosomal rearrangements in ALK have been detected in different types of human cancer and, together with other oncogenic evidence, ALK has been adopted as another attractive target for cancer treatment with more than ten molecules currently undergoing clinical trials [66].

Crizotinib (Xalkori®, Pfizer) was the first ALK inhibitor approved (Figure 8A), for the treatment of late-stage lung cancer, anaplastic large cell lymphoma, and neuroblastoma. It was also the first drug specifically targeting non-small-cell lung carcinoma (NSCLC) patients. Besides ALK, crizotinib also acts on ROS proto-oncogene 1-encoded kinase (ROS1) of the tyrosine kinase insulin receptor class and MET proto-oncogene-encoded kinase (MET) of the hepatocyte growth factor receptor (HGFR) class [67,68]. A co-crystal structure with ALK showed that crizotinib binds with the ATP-binding pocket in a type I mode. The aminopyridine core sits at the adenine pocket and makes hydrogen bonds with hinge residues Glu1197 and Met1199. The methyl group of the benzyloxy moiety binds with a small hydrophobic pocket under the N-lobe. The 2,6-dichloro substituent of the terminal benzyl handle contributes to the high potency against c-MET. Overall, crizotinib does not fully utilize the structural features of the ATP-binding pocket of ALK, which partially explained its poor selectivity [68] (Figure 8B,C).

Ceritinib (Zykadia®, Novartis) was developed as a second-generation ALK inhibitor for the treatment of NSCLC with developed resistance to crizotinib due to rearrangements of the ALK gene [69] (Figure 8D). It has been shown that ceritinib potently overcomes ALK bearing L1196M, G1269A, I1171T, and S120Y mutations, but not ALK with G1202R and F1174C mutations [70]. The ALK–ceritinib co-crystal structure showed a binding mode similar to that of the ALK–crizotinib complex with the DFG motif adopting the in conformation [70]. The conserved hydrogen bonds were formed between the 2,4-diaminopyrimidine core and hinge residue Met1199. The isopropylsulfonylphenyl handle binds deeper inside the hydrophobic pocket and the anchor-shaped terminal 2-isopropoxy-3-(piperidin-4-yl)phenyl group lies in the interface between the solvent and the ATP-binding pocket.

MET, or c-MET, is a tyrosine kinase that is the only know receptor of HGF [71,72]. MET-induced activation of signaling cascades recruits downstream effectors including SRC, PI3K, tyrosine phosphatase SRC homology 2 domain-containing phosphatase 2 (SHP2), and the transcription factor STAT-3, regulating proliferation, motility, migration, and a wide range of other cellular activities [73]. Given its pivotal role in cancer development and progression, MET has been promoted as a versatile candidate for cancer treatment [74]. Besides a small group of selective MET inhibitors, most current MET inhibitors target multiple kinases, including the two approved molecules: the abovementioned crizotinib and the dual MET and VEGFR2 inhibitor cabozantinib (Cometriq®, Exelixis). A recent study showed that cabozantinib overcomes

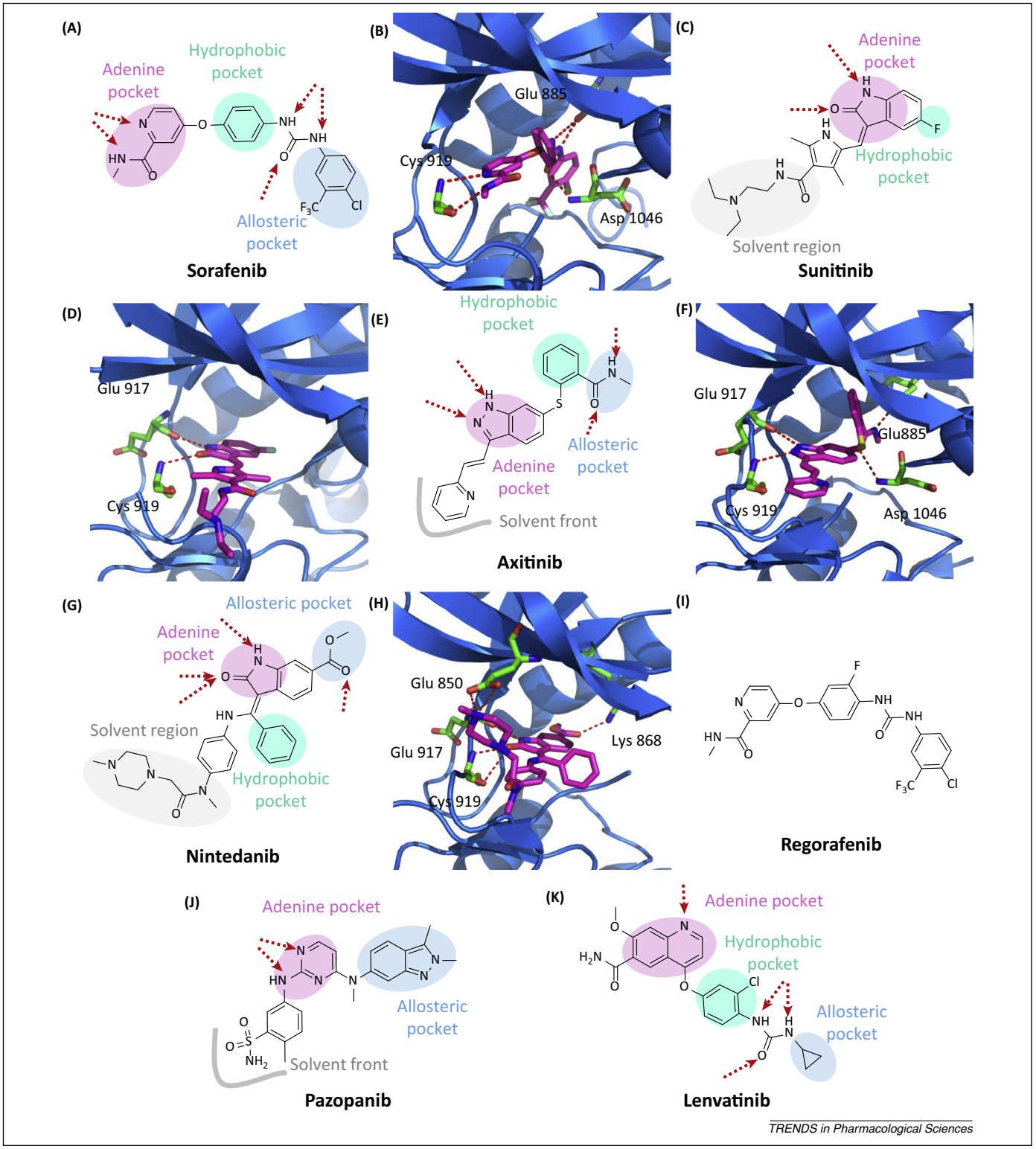

Figure 7. Small-molecule kinase inhibitors binding to the vascular endothelial growth factor receptor (VEGFR). **(A)** Chemical structure of sorafenib and its depicted binding mode with VEGFR2. **(B)** Sorafenib co-crystal structure with VEGFR2 [Protein Data Bank (PDB) ID: 4ASD, 2.03 Å]. **(C)** Chemical structure of sunitinib and its depicted binding mode with VEGFR2. **(D)** Sunitinib co-crystal structure with VEGFR2 (PDB ID: 4AGD, 2.81 Å). **(E)** Chemical structure of axitinib and its depicted binding mode with VEGFR2. **(F)** Axitinib co-crystal structure with VEGFR2 (PDB ID: 4AG8, 1.95 Å). **(G)** Chemical structure of nintedanib and its depicted binding mode with VEGFR2. **(H)** Nintedanib co-crystal structure with VEGFR2 (PDB ID: 3C7Q, 2.10 Å). **(I)** Chemical structure of regorafenib. **(J)** Chemical structure of pazopanib and its proposed binding mode with VEGFR2 based on the crystal structure of PDB ID: 3CJG (2.25 Å). **(K)** Chemical structure of lenvatinib and its depicted binding mode with VEGFR2. Small-molecule inhibitors are shown in magenta backbone, hydrogen bonds are indicated by red broken lines, and residues that interact with inhibitors through hydrogen bonds are shown in green backbone.

crizotinib resistance stemming from acquired mutations in ROS1 [75].

The MET–crizotinib complex showed a type I binding mode similar to that of the ALK–crizotinib complex with the DFG adopting an in conformation [68] (Figure 9A). The hinge hydrogen bonds involving the aminopyridine core are preserved while the 3-fluoro-2,6-dichlorobenzyl moiety binds in a large hydrophilic pocket adjacent to the solvent

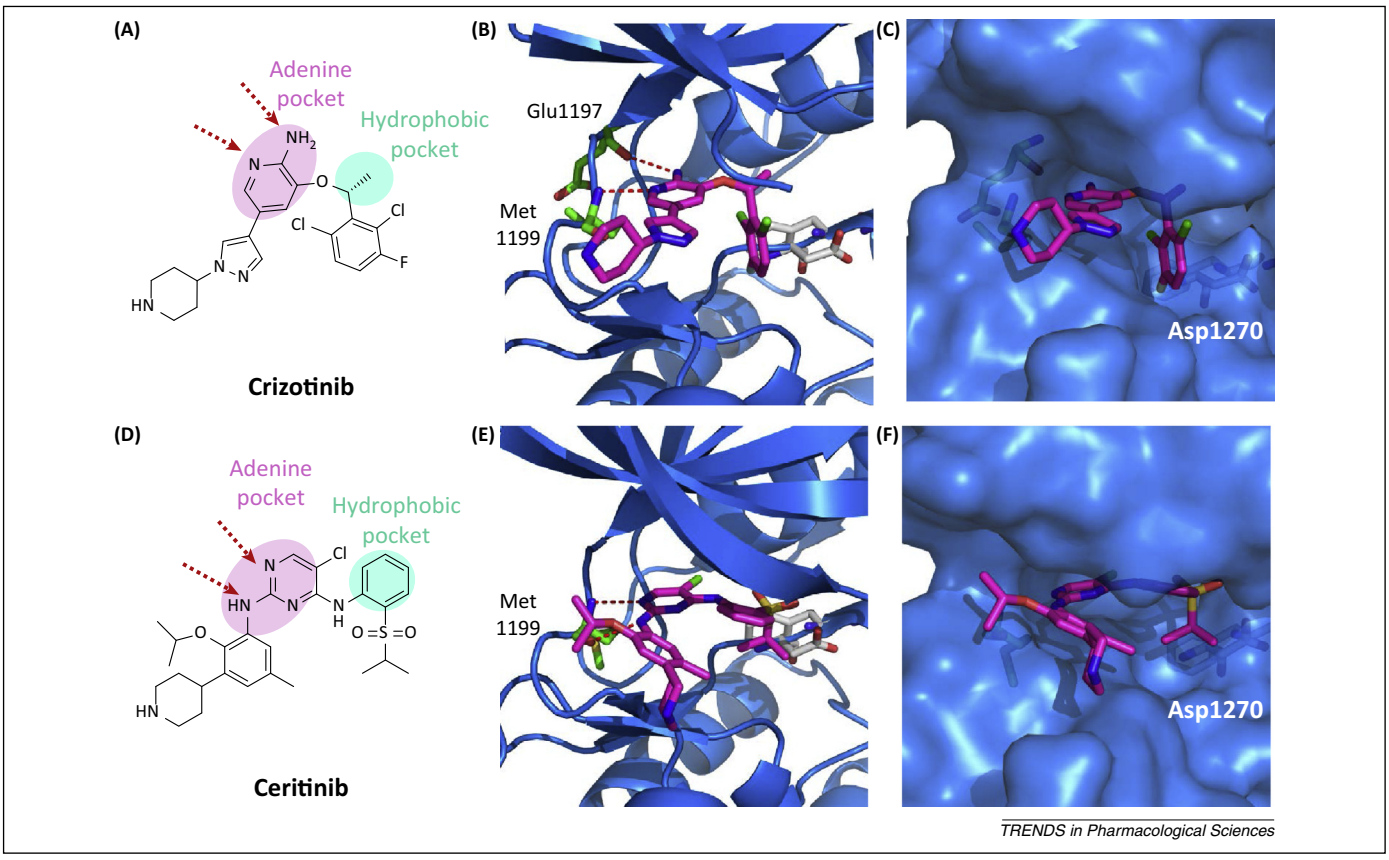

Figure 8. Small-molecule kinase inhibitors binding to anaplastic lymphoma kinase (ALK). **(A)** Chemical structure of crizotinib and its depicted binding mode with ALK. **(B,C)** Crizotinib co-crystal structure with ALK [Protein Data Bank (PDB) ID: 2XP2, 1.9 Å]. **(D)** Chemical structure of ceritinib and its depicted binding mode with ALK. **(E,F)** Ceritinib co-crystal structure with ALK (PDB ID: 4MKC, 2.01 Å). Small-molecule inhibitors are shown in magenta backbone, hydrogen bonds are indicated by red broken lines, residues that interact with inhibitors through hydrogen bonds are shown in green backbone, and residues of the Asp-Phe-Gly (DFG) motif are shown in white backbone.

front (Figure 9B,C). Despite the absence of a MET co-crystal structure with cabozantinib (Figure 9D), the MET complex with the compound DWF (Figure 9E), a closely related analog, showed a potent type II binding mode. The aminopyrimidine core and the connecting fluorophenyl group lie in the adenine pocket and hydrophobic pocket utilized by crizotinib, respectively. The DFG-out conformation opens a hydrophobic allosteric pocket that is occupied by the terminal 4-fluorophenyl group. Besides forming a hydrogen bond with the N-lobe residue Lys1110, the cyclopropane–dicarboxamide link binds with an allosteric channel interacting directly with the DFG residue Asp1222 through the formation of a hydrogen bond. The sulfonylphenyl group extends to the solvent and forms hydrogen bonds with C-lobe residues Asp1164 and Asn1167 (Figure 9F,G).

Approved irreversible protein kinase inhibitors

The EGFR inhibitor afatinib was the first clinically approved irreversible kinase inhibitor, followed shortly by ibrutinib in November 2013. The approval of these two molecules validates the strategy of incorporating Michael acceptor functionality in small-molecule inhibitors to form a covalent bond with a cysteine residue in the active site of kinases. This type of irreversible inhibitor is expected to achieve greater specificity and potency, although concerns have been raised regarding potential toxicities.

Co-crystal structures of both wild type EGFR–afatinib and mutant T790M EGFR–afatinib showed a type I binding mode that has a high degree of similarity with other approved reversible EGFR inhibitors sharing the same anilinoquinazoline core (Figure 10A). A conserved hydrogen bond is formed between hinge residue Met793 and the quinazoline ring. Electron density indicated the formation of a covalent C–S bond (1.8 Å) between the enone tail and Cys797 at the edge of the active site in the C-lobe [76] (Figure 10B,C).

Ibrutinib (Imbruvica®, Pharmacyclics Inc.) is a NRTK inhibitor that targets Bruton's tyrosine kinase (BTK), which is an essential component of B-cell receptor signaling in regulating the survival and proliferation of chronic lymphocytic leukemia (CLL) cells [77]. It was approved for the treatment of mantle cell lymphoma in November 2013 and then for CLL in February 2014 [78]. Global sales of Ibrutinib are expected to reach US$9 billion in 2020 [79]. A co-crystal structure of BTK with ibrutinib remains to be reported, but one of BTK with a close analog of ibrutinib, B43, could be used to deduce a general binding mode between BTK and ibrutinib [80] (Figure 10D,E). B43 binds to the ATP site with the activation loop displaying a 'DFG-in' conformation. The 4-amino pyrrolopyrimidine of B43 mimics the adenine ring of ATP, making several hydrogen bond interactions with the hinge region. The terminal phenyl group is twisted out of the connecting phenyl ether

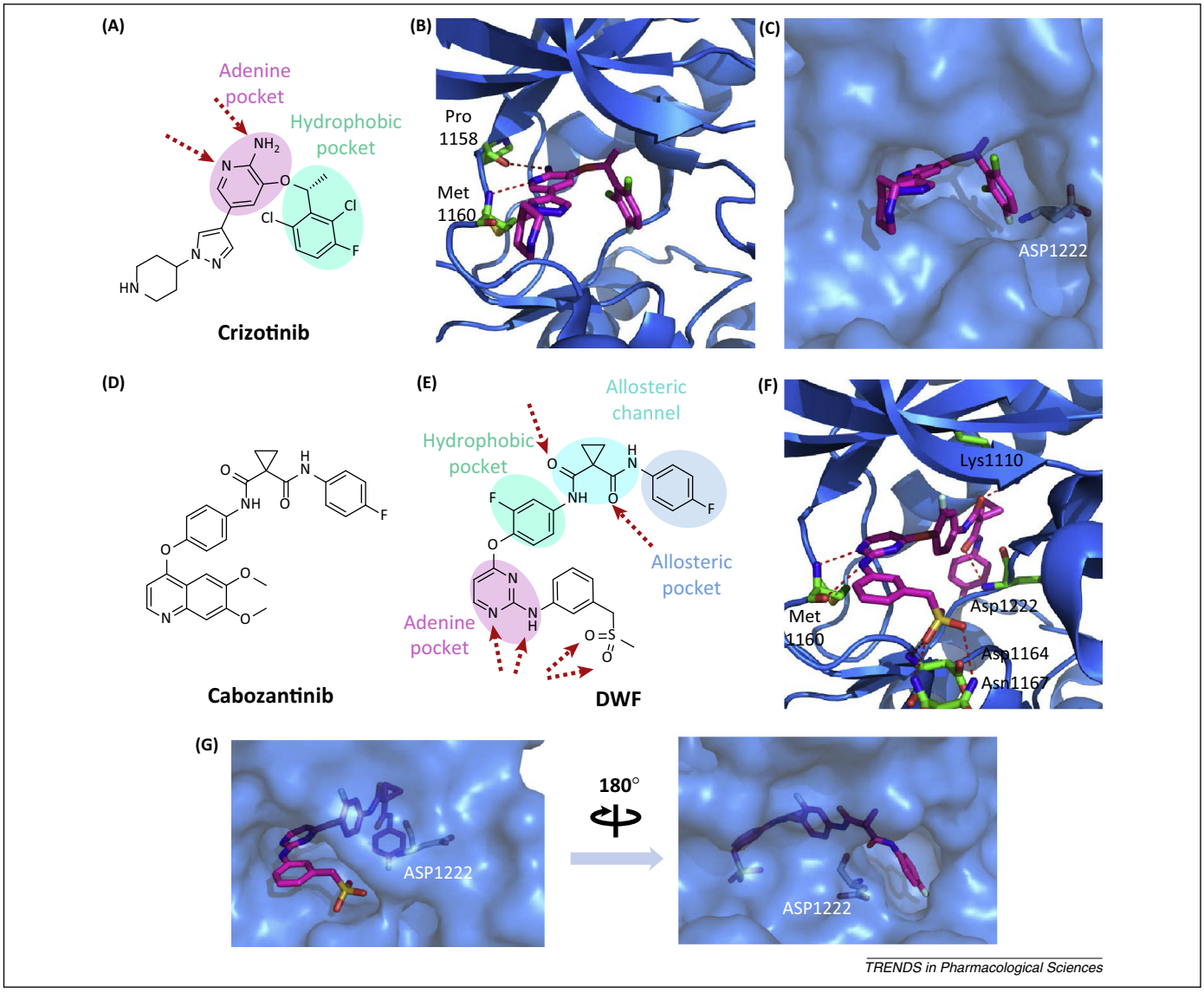

Figure 9. Small-molecule kinase inhibitors binding to MET. **(A)** Depicted binding mode of crizotinib with MET. **(B,C)** Crizotinib co-crystal structure with MEK [Protein Data Bank (PDB) ID: 2WGJ, 2.0 Å]. **(D)** Chemical structure of cabozantinib. **(E)** Chemical structure of compound DWF (name derived from PDB ligand identifier code) and its depicted binding mode with MET. **(F,G)** Cabozantinib co-crystal structure with MET (PDB ID: 4MXC, 1.63 Å). Small-molecule inhibitors are shown in magenta backbone, hydrogen bonds are indicated by red broken lines, residues that interact with inhibitors through hydrogen bonds are shown in green backbone, and the Asp residue of the Asp-Phe-Gly (DFG) motif is shown in white backbone.

plane to enter a hydrophobic pocket mainly formed by the N-lobe residues. The phenoxyphenyl group forms π-stacking interactions with residues of this hydrophobic pocket. The cyclopentyl group of B43 extends toward Cys481 of the activation loop (Figure 10F). In the case of ibrutinib, the cyclopentyl group is replaced with an *N*-acryloylpiperidine group that acts as a Michael acceptor in reaction with the vicinal cysteine.

Approved serine/threonine kinase inhibitors

The serine/threonine kinase B-Raf, one of the three isoforms of the Raf family, has been established as an attractive anticancer target [81]. Replacement of Val600 with Glu600 within the activation loop of the kinase domain accounts for 90% of B-Raf mutations [82], resulting in destabilization of the inactive conformation, elevated activation of the MAPK pathway, and enhanced promotion of cell survival and proliferation. Efforts in developing small-molecule kinase inhibitors led to the approved of the first B-Raf inhibitor, vemurafenib (Zelboraf®, Roche), in 2011 for the treatment of metastatic melanoma and thyroid tumors [81], followed by the approved of dabrafenib (Tafinlar®, GlaxoSmithKline) in 2013. The tyrosine kinase inhibitor sorafenib has also been shown to inhibit Raf kinases including C-Raf and B-Raf [82].

Vemurafenib (Figure 11A) was developed using a fragment-based drug discovery strategy. The V600E B-Raf–vemurafenib co-crystal structure showed a type I binding mode. Vemurafenib occupies the ATP-binding site with a DFG-in conformation, enabling the formation of hydrogen bond interactions between the sulfonamide moiety and the DFG residues. Hydrogen bonds are also formed between the pyrrolopyridine core and hinge residue Cys532 and Gln530, mimicking that of the adenine core of ATP. The

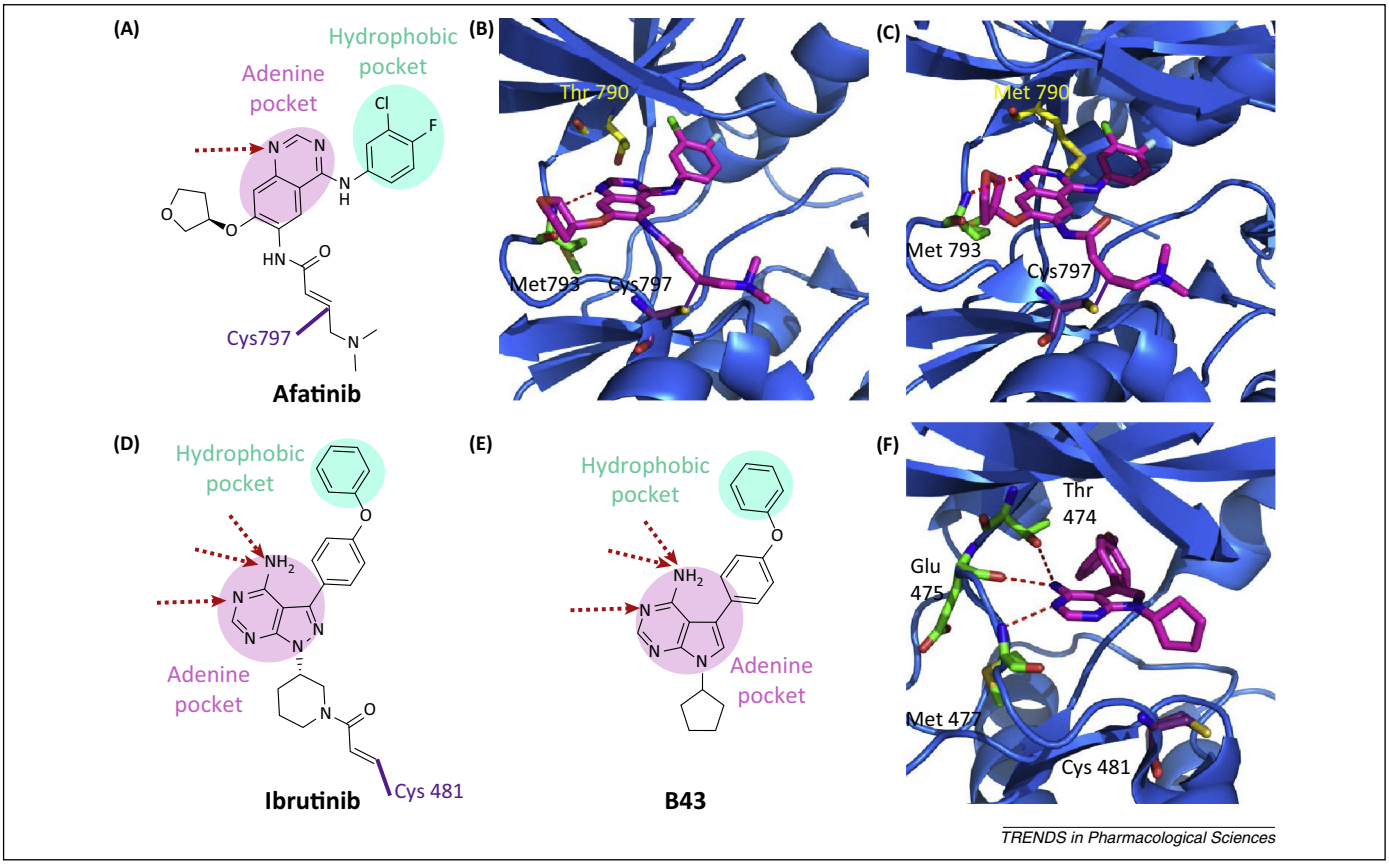

Figure 10. Binding mode of irreversible small-molecule kinase inhibitors. **(A)** Chemical structure of afatinib and its depicted binding mode with the epidermal growth factor receptor (EGFR). **(B)** Afatinib co-crystal structure with wild type EGFR [Protein Data Bank (PDB) ID: 4G5J, 2.80 Å]. **(C)** Afatinib co-crystal structure with mutant T790M EGFR (PDB ID: 4G5P, 3.17 Å). **(D)** Chemical structure of ibrutinib and its proposed binding mode with Bruton's tyrosine kinase (BTK). **(E)** Chemical structure of compound B43 and its depicted binding mode with BTK. **(F)** B43 co-crystal structure with BTK (PDB ID: 3GEN, 1.60 Å). Wild type and mutant residue 790 of the EGFR is shown in yellow backbone, small-molecule inhibitors are shown in magenta backbone, hydrogen bonds are indicated by red broken lines, residues that interact with inhibitors through hydrogen bonds are shown in green backbone, covalent bonds are indicated by purple unbroken lines, and the cysteine residue contributing to the formation of a covalent bond is shown in purple backbone.

terminal 4-chlorophenyl group is exposed to the solvent front. In addition, an outward shift of the regulatory αC-helix caused by vemurafenib binding to the kinase was observed [83] (Figure 11B,C). Although no co-crystal structure of dabrafenib (Figure 11D) with B-Raf has yet been obtained, a complex of mutant V600E B-Raf with compound **20** (Figure 11E), a diarylthiazole derivate of dabrafenib, showed an interacting mode that shares features of type I binding. Compound **20** binds the ATP site with the activation loop adopting a DFG-in conformation. Hydrogen bond interactions with the hinge and the DFG residues were preserved through the acetamidopyridine handle and the sulfonamide moiety, respectively. The 2,5-difluorophenyl moiety extends inside a hydrophobic pocket, or Ras-selective pocket, which is formed through the outward movement of the αC-helix. The thiazole core occupies the ribose pocket, which is barely utilized by other kinase inhibitors, and the cyclopropylpiperidine tail attached to the thiazole core extends toward the solvent environment [84] (Figure 11F). A mechanistic study indicated that the activation loop of B-Raf is held in an inactive state by association with the P-loop. Mutations of the activation loop or the P-loop disrupt the inactive conformation and convert B-Raf into its active conformation. Co-crystal structures of the tyrosine kinase inhibitor sorafenib with both wild type and mutant B-Raf showed different binding modes when the Val599 of the activation loop is mutated to Glu599 [82] (Figure 11G–I).

Along the MAPK pathway, MEK is another target for which a considerable number of small-molecule inhibitors have been identified [85], including the only approved molecule, trametinib (Mekinist®, GlaxoSmithKline) (Figure 12A). Trametinib was developed based on a high-throughput screening (HTS) hit that bears the same pyridopyrimidinetrione core. SAR studies driven by growth inhibitory activity against cancer cell lines led to the discovery of trametinib [86], whose target was then confirmed as MEK1 and MEK2 guided by the structural features of known MEK inhibitors. The co-crystal structure of MEK1 with an analog of trametinib, TAK-733 (Figure 12B), showed a type III binding mode. The pyridopyrimidinedione core lies in an allosteric pocket adjacent to the ATP-binding pocket with the pyridine oxygen forming hydrogen bonds with Val211 and Ser212 and the pyrimidine oxygen interacting with Lys97. The 2-fluoro-4-iodoaniline moiety functions as a recognition motif for the hydrophobic pocket of the MEK allosteric site. The hydroxyl groups of the terminal dihydroxypropyl chain forms hydrogen bonds with both the ATP phosphate and Lys97 [87] (Figure 12C). A combination strategy of the B-Raf

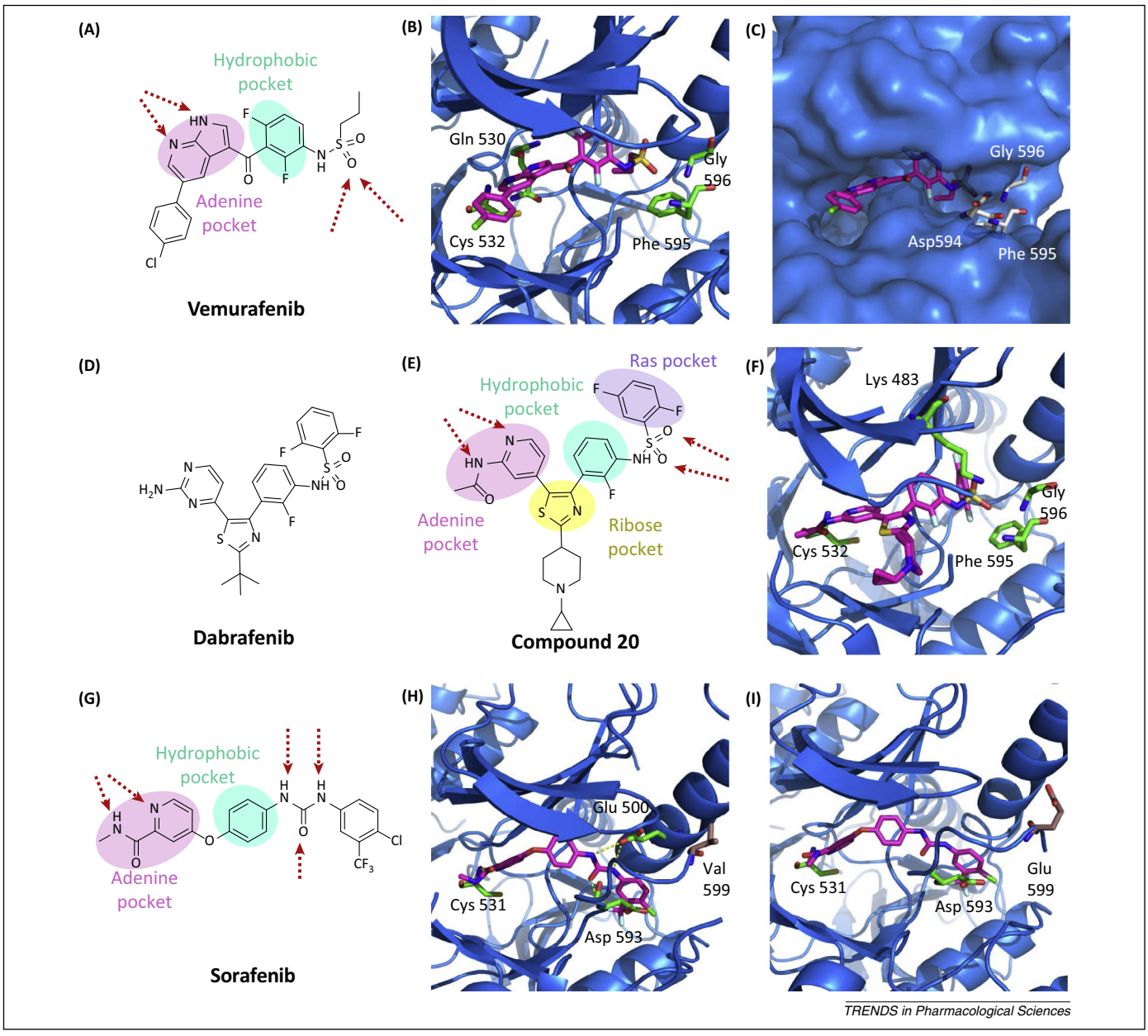

Figure 11. Structures of approved small-molecule kinase inhibitors binding to serine/threonine kinase B-Raf. **(A)** Chemical structure of vermurafenib and its depicted binding mode with mutant V600E B-Raf kinase. **(B)** Vemurafenib co-crystal structure with V600E B-Raf [Protein Data Bank (PDB) ID: 3OG7, 2.45 Å]. **(C)** Surface show of the vemurafenib–V600E B-Raf complex with the residues of the Asp-Phe-Gly (DFG) motif highlighted in white backbone (PDB ID: 3OG7, 2.45 Å). **(D)** Chemical structure of dabrafenib. **(E)** Chemical structure of the dabrafenib derivative compound **20** and its depicted binding mode with mutant V600E B-Raf. **(F)** Compound **20** co-crystal structure with V600E B-Raf (PDB ID: 4CQE, 2.30 Å). **(G)** Chemical structure of sorafenib and its depicted binding mode with wild type B-Raf. **(H)** Sorafenib co-crystal structure with wild type B-Raf (PDB ID: 1UWH, 2.95 Å). **(I)** Sorafenib co-crystal structure with mutant V599E B-Raf; mutated residue Glu599 is shown in brown backbone (PDB ID: 1UWJ, 3.5 Å). Small-molecule inhibitors are shown in magenta backbone, hydrogen bonds are indicated by red broken lines, and residues that interact with inhibitors through hydrogen bonds are shown in green backbone.

inhibitor dabrafenib with the MEK inhibitor trametinib, approved for the treatment of mutant V600E/K metastatic melanoma by the FDA in early 2014, has been used to overcome the drug resistance that occurs within about half a year after applying B-Raf inhibitors [88,89].

The serine/threonine kinases Akt and mammalian target of rapamycin (mTOR) of the PI3K/Akt/mTOR pathway are also promising targets [90]. Although no small-molecule kinase inhibitors have been approved for either Akt or mTOR, there is a pipeline of candidates currently undergoing various clinical trials in different phases [91]. For mTOR inhibitors, three natural-product-based macrolides – sirolimus, temsirolimus, and everolimus – were approved for clinical use in 1999, 2007, and 2009, respectively [90].

Cyclin-dependent kinases (CDKs) represent another group of serine/threonine kinases that have been studied as targets for therapeutic intervention in various types of cancer and other proliferative diseases [92]. Intensive efforts have been made in the past two decades to discover inhibitors with varied selectivity against the 11 isoforms of CDKs, resulting in the emergence of approximately 20 CDK inhibitors currently in various clinical trials [93]. The first CDK inhibitor, palbociclib (Ibrance®, Pfizer),

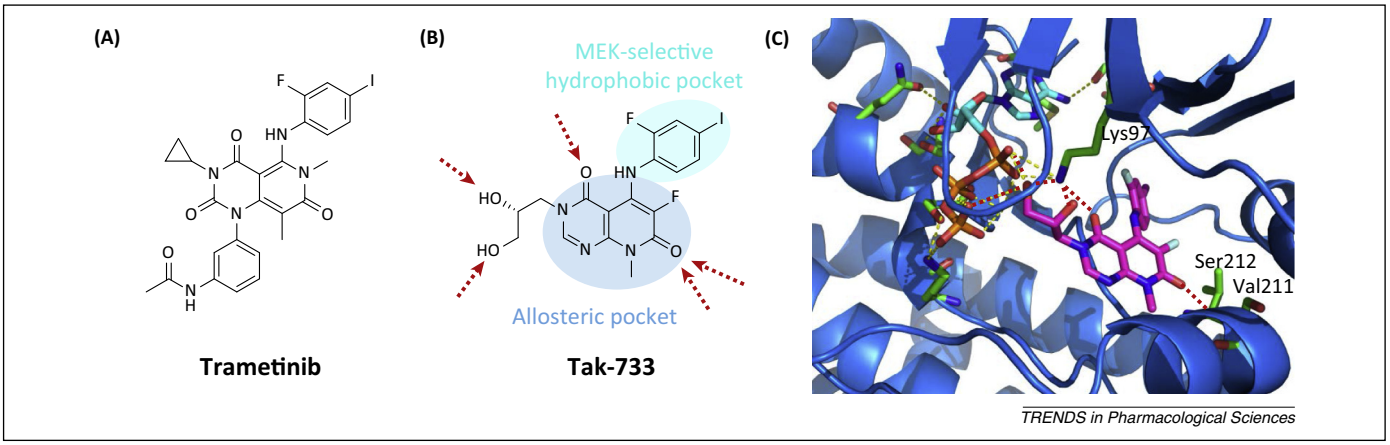

Figure 12. MEK kinase inhibitor binding mode. **(A)** Chemical structure of trametinib. **(B)** Chemical structure of Tak-733 and its depicted binding mode with MEK1. **(C)** Tak-733 co-crystal structure with MEK1 [Protein Data Bank (PDB) ID: 3PP1, 2.70 Å]. ATP is shown in cyan backbone and Tak-733 in magenta backbone, hydrogen bonds are indicated by red broken lines, and residues that interact with ATP and Tak-733 through hydrogen bonds are shown in green backbone.

was approved in February 2015 for the treatment of breast cancer.

Palbociclib is a selective CDK4 and CDK6 inhibitor (Figure 13A). Due to conformational differences in the hinge region of CDKs, the selectivity profiles of CDK inhibitors are closely connected with their binding orientations [94]. The co-crystal structure of palbociclib with CDK6 showed a tight binding mode in which hydrogen bonds are formed between the hinge residue Val101 and the aminopyrimidine moiety and between the DFG residue Asp163 and the 6-acetyl group. The 5-methyl and 6-acetyl groups fully occupy a hydrophobic pocket in the back of the ATP-binding site. The piperazinylpyridinylamino substituent at the 2-position of the pyrido[2,3-*d*]pyrimidinone core binds into a specificity pocket facing to the solvent front (Figure 13B,C). Overall, palbociclib binds tightly into CDK6 and adopts a comparatively rigid orientation compared with other pan-CDK inhibitors due to the abovementioned binding features [94].

Approved lipid kinase inhibitors

Lipid kinases, such as PI3Ks, were discovered as early as the 1980s [95]. It has been convincingly established that activation and mutation of PI3Ks and other key components of this signaling pathway play key roles in various stages of tumor development [96]. Considerable efforts from both academia and industry have been involved in the development of small-molecule lipid kinases since the 1980s, but the clinical success of these inhibitors was minimal until the approval of the first lipid kinase inhibitor, idelalisib (Zydelig®, Gilead Sciences), for CLL in combination with monoclonal antibody rituximab in July 2014 [97]. The approval of idelalisib, together with the BTK inhibitor ibrutinib, provides encouraging an transformation of the treatment of CLL [98].

Idelalisib is a PI3Kδ inhibitor [99] (Figure 14A). The crystal complex of PI3Kδ with idelalisib revealed a type II binding that is similar to that of another selective PI3Kδ inhibitor, PIK39 [100]. Idelalisib adopts a propeller-shaped conformation with the DFG motif posing in an 'out' conformation [101]. The 5-fluoroquinazolinone moiety squeezes into an induced hydrophobic specificity pocket. The ethyl group binds in a hydrophobic pocket and the phenyl group extends into a hydrophobic region that is close to the solvent front. The hinge hydrogen bond, which is a highly conserved feature for PI3K inhibition [102], is formed

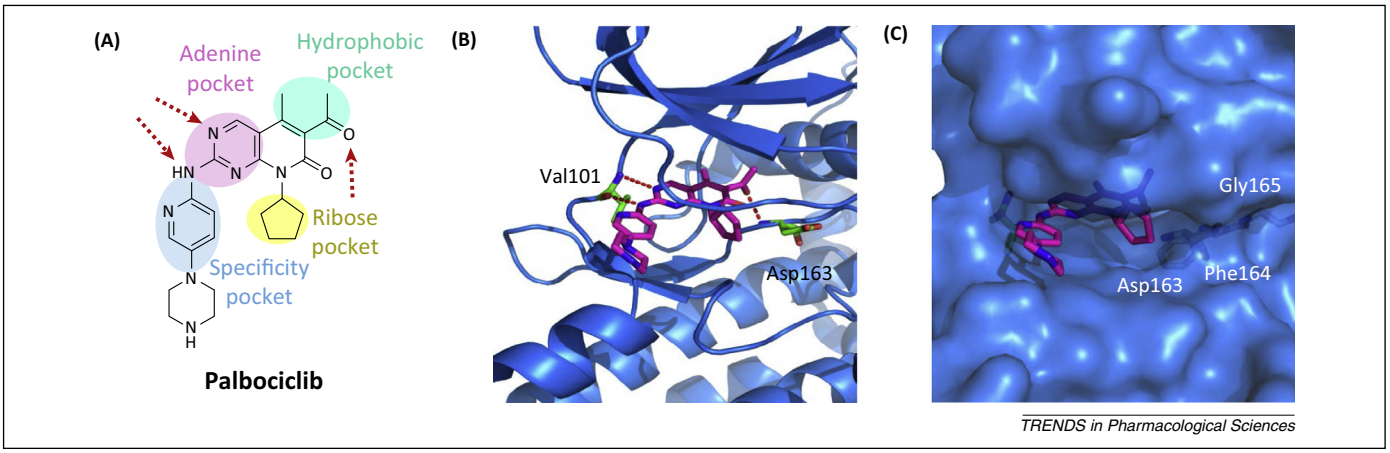

Figure 13. Cyclin-dependent kinase (CDK) inhibitor palbociclib. **(A)** Chemical structure of palbociclib and its depicted binding mode with CDK6. **(B,C)** Palbociclib co-crystal structure with CDK6 [Protein Data Bank (PDB) ID: 2EUF, 3.0 Å]. Palbociclib is shown in magenta backbone, hydrogen bonds are indicated by red broken lines, residues that interact with inhibitors through hydrogen bonds are shown in green backbone, and residues of the Asp-Phe-Gly (DFG) motif are shown in white backbone.

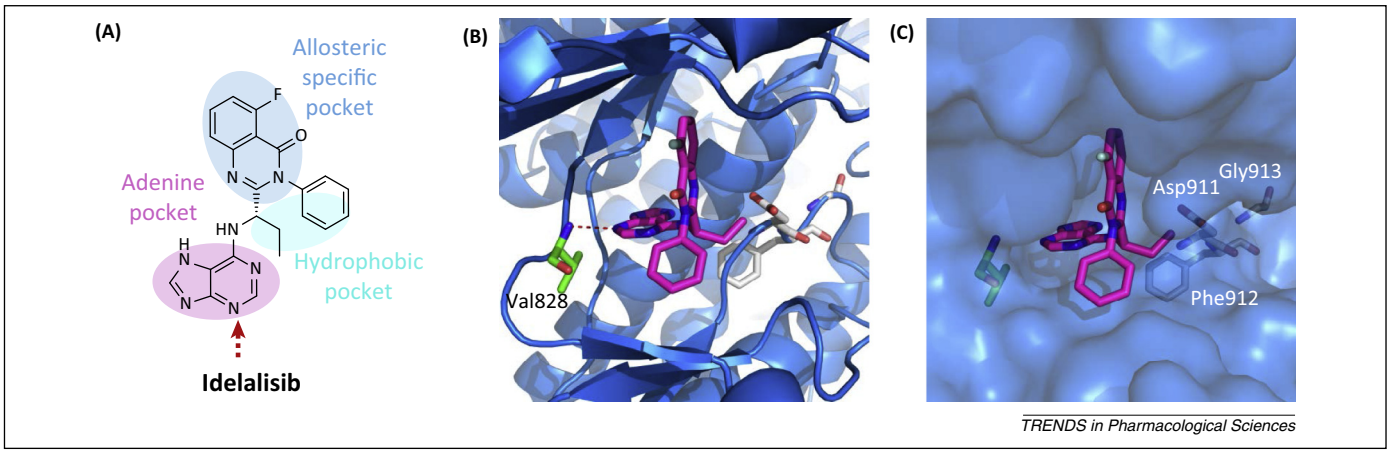

Figure 14. Phosphoinositide 3-kinase delta (PI3Kδ) inhibitor idelalisib. **(A)** Chemical structure of idelalisib and its depicted binding mode with PI3Kδ. **(B,C)** Idelalisib co-crystal structure with PI3Kδ [Protein Data Bank (PDB) ID: 4XE0, 2.43 Å]. Idelalisib is shown in magenta backbone, hydrogen bond is indicated by a red broken line, and residues of the Asp-Phe-Gly (DFG) motif are shown in white backbone.

between Val828 and the purine moiety that occupies the adenine pocket [101] (Figure 14B,C). Besides being approved for CLL, idelalisib has also been granted accelerated approval for relapsed follicular B-cell non-Hodgkin lymphoma and relapsed small lymphocytic lymphoma [103,104].

More than 20 other PI3K inhibitors – including single-isoform inhibitors such as the PI3Kα inhibitor buparlisib (Phase III, Novartis), selective-isoform inhibitors, dual inhibitors of PI3K and mTOR, and pan-class I PI3K inhibitors – are in development for cancers and inflammatory diseases [102]. However, the clinical data accumulated so far suggest that PI3K inhibitors have limited single-agent activity [105], possibly due to negative feedback inhibition and the resulting reactivation of downstream receptor signaling [106,107]. Thus, rational combination strategies using monoclonal antibodies, tyrosine kinase inhibitors, and serine/threonine kinase inhibitors are needed to assist the clinical use of PI3K inhibitors.

Limitations and challenges

Kinase-based drug discovery has achieved dramatic progress in the past 15 years. Although kinase inhibition represents a young therapeutic strategy compared with other, traditional tactics targeting, for example, G protein-coupled receptors (GPCRs), membrane channels and transporters, and protease, an analysis of FDA-approved cancer drugs since the 1980s reveals that kinases have already overtaken GPCRs as the most sought-after cellular targets for cancer treatment [108]. Our analysis of all FDA-approved small-molecule kinase inhibitors with a focus on binding mechanism and structural features reveals some general conclusions that form the current landscape of developing kinase inhibitors and reflects several significant challenges despite the achieved advances.

First, only a small subset of the human kinome has been studied. Most kinase inhibition efforts are limited to a select group of kinases that belong to the tyrosine kinase group, although promising results are emerging for the inhibition of kinases in tyrosine kinase-like (TKL) groups, including CDK, MAPK, GSK3, and CLK kinase (CMGC), PKA, PKG, and PKC kinase (AGC), and the calcium/calmodulin-dependent protein kinases (CAMKs) in recent years. This imbalance is clearly illustrated by the fact that inhibitors of three groups of tyrosine kinases – BCR-Abl, ErbBs, and VEGFRs – account for 18 of the 27 approved protein kinase inhibitors.

Second, in contrast to protein kinase inhibitors, only one lipid kinase inhibitor is currently on the market. Although lipid kinase inhibitors were reported as early as the 1990s and various clinical and preclinical lipid kinase inhibitors have been published [102], few have showed sufficient activity when used in single-agent trials.

Third, despite the fact that kinase signaling cascades regulate diverse cellular activities related to, for example, inflammatory indications, CNS disorders, cardiovascular disease, and diabetes in addition to cancer, most of the currently available inhibitors, including 26 of the 28 approved kinase inhibitors, were developed mainly for cancer treatment.

Fourth, many of the current kinase inhibitors were designed based on previously approved compounds, as shown by the high structural similarity among approved ErbB inhibitors; for example, five ErbB inhibitors share the same 4-(arylamino)quinazoline core with different 6 and/or 7 substituents. Consequently, only a small subset of chemotypes are being investigated, which is clearly reflected by the limited number of moieties that are incorporated in the approved molecules.

Fifth, most inhibitors function as reversible inhibitors binding in the ATP-binding pocket and, due to the high sequence similarity around the ATP-binding pockets of kinases, it has been a daunting task to develop kinase inhibitors with potent inhibition against desirable targets and minimal interactions with off-targets.

Sixth, closely connected with the previous point, a large number of inhibitors interact with more than one target. By contrast, few absolute-selective inhibitors, which might be evaluated as dual- or multiple-target inhibitors if a more comprehensive screening assay was used [109], have been identified so far.

Future directions

Based on the current trends discussed above, some challenging questions that might serve as directions for future development of small-molecule kinase inhibitors and push the boundary of the research in this field need to be addressed appropriately.

First, the fact that current kinase inhibitors focus on only a small subset of the human kinome indicates that many kinases are neglected. Thus, there is a need to develop tools and selective probes to uncover the functions of these unknown kinases [110], which might serve as new targets for small-molecule inhibitors. It is encouraging to see the approval of a first inhibitor targeting certain kinases in the past 3 years, like trametinib as the first approved MEK inhibitor in 2013, ibrutinib as the first approved BTK inhibitor in 2013, and palbociclib as the first approved CDK inhibitor in 2015.

Second, although significant efforts have been devoted to the development of lipid kinase inhibitors, the progress achieved is not as obvious as for protein kinase inhibitors. The approval of the first and only lipid kinase inhibitor idelalisib in 2014 added support to the strategy of using lipid kinase inhibitors as anticancer agents, especially in combination with other cancer treatment agents and methods. Considering the pivotal roles of lipid kinases such as PI3Ks in cellular cascades, it is reasonable to expect research on small-molecule lipid kinase inhibitors, for indications including not only cancer but also inflammation, to be a promising direction in this field.

Third, except for being utilized in the prevalent theme for cancer treatment, kinase inhibitors have great potential in the treatment of nonlethal chronic diseases such as cardiovascular and CNS disorders. The successful approval of tofacitinib established the concept for the treatment of arthritis. Even for cancer treatment, more knowledge needs to be gained to further understand the multifaceted cancer biology.

Fourth, more pharmacophores need to be explored to diversify the scaffolds of kinase inhibitors. Most currently approved kinase inhibitors were discovered based on hits from HTS, while HTS is becoming increasingly less effective since most useful scaffolds have already been retrieved from available compound libraries. So, there is an urgent need to diversify the molecules in compound libraries for screening. Natural products, which usually contain pharmacophores and scaffolds that differ from most synthetic kinase inhibitors, could be a useful source to inspire the construction of libraries with expanded structural diversity.

Fifth, despite the fact that most approved kinase inhibitors are type I or II reversible inhibitors, the success of afatinib and ibrutinib represents a strong stimulator to rekindle the idea of targeting kinases with irreversible inhibitors. However, type III and IV inhibitors might show different efficacies and selectivities compared with type I and II inhibitors. In short, novel mechanisms of action need to be explored.

Sixth, the selectivity issue of kinase inhibitors has always been a controversial area. Early promiscuous inhibitors (e.g., staurosporine) and later pan-selective inhibitors have functioned as useful tools in oncology. Highly selective kinase inhibitors were actively sought after until the recent theory that inhibitors with favorable selectivity or multitarget selectivity might be more suitable for cancer treatment became increasingly widely accepted. It has become clear that kinase inhibitors do not have to be absolute selective; a favorable selectivity profile is needed to balance efficacy and toxicity.

Concluding remarks

Groundbreaking understanding of cellular signaling cascades at the molecular level has led to major advances in kinase research over the past decades. The dramatic progress in applying the strategy of targeted kinase inhibition in the past 15 years has been highlighted by the successful approval of no less than 28 small-molecule kinase inhibitors. An analysis based on co-crystal structures of all approved inhibitors with a focus on binding mechanism and structural features is presented here to provide an updated overview of the achievements and shape current limitations and challenges in this rapidly evolving field. Future directions that may lead to the discovery of small-molecule kinase inhibitors with novel functional mechanisms, new therapeutic indications, distinct structures, and different selectivity and pharmacological profiles are also proposed. Although the current task of developing small-molecule kinase inhibitors is highly interdisciplinary, the ultimate answer to the question of which type of kinase inhibitor is most useful will have to come from the accumulated clinical data of the approved molecules discussed in this review.

Acknowledgements

The Lundbeck Foundation (R140-2013-13835) is gratefully acknowledged for financial support. The authors thank Professor David A. Tanner for proofreading the manuscript.

Appendix A. Supplementary data

Supplementary data associated with this article can be found, in the online version, at http://dx.doi.org/10.1016/j.tips.2015.04.005.

References

1 Johnson, L.N. and Lewis, R.J. (2001) Structural basis for control by phosphorylation. *Chem. Rev.* 101, 2209–2242
2 Adams, J.A. (2001) Kinetic and catalytic mechanisms of protein kinases. *Chem. Rev.* 101, 2271–2290
3 Rask-Andersen, M. *et al.* (2014) Advances in kinase targeting: current clinical use and clinical trials. *Trends Pharmacol. Sci.* 35, 604–620
4 Huang, M. *et al.* (2014) Molecularly targeted cancer therapy: some lessons from the past decade. *Trends Pharmacol. Sci.* 35, 41–50
5 Ma, W.W. and Adjei, A.A. (2009) Novel agents on the horizon for cancer therapy. *CA Cancer J. Clin.* 59, 111–137
6 Sun, C. and Bernards, R. (2014) Feedback and redundancy in receptor tyrosine kinase signaling: relevance to cancer therapies. *Trends Biochem. Sci.* 39, 465–474
7 Clark, J.D. *et al.* (2014) Discovery and development of Janus kinase (JAK) inhibitors for inflammatory diseases. *J. Med. Chem.* 57, 5023–5038
8 Barnes, P.J. (2013) New anti-inflammatory targets for chronic obstructive pulmonary disease. *Nat. Rev. Drug Discov.* 12, 543–559
9 Muth, F. *et al.* (2015) Tetra-substituted pyridinylimidazoles as dual inhibitors of p38α mitogen-activated protein kinase and c-Jun N-terminal kinase 3 for potential treatment of neurodegenerative diseases. *J. Med. Chem.* 58, 443–456
10 Kikuchi, R. *et al.* (2014) An antiangiogenic isoform of VEGF-A contributes to impaired vascularization in peripheral artery disease. *Nat. Med.* 20, 1464–1471

11 Banks, A.S. *et al.* (2015) An ERK/Cdk5 axis controls the diabetogenic actions of PPARγ. *Nature* 517, 391–395
12 Burnett, G. and Kennedy, E.P. (1954) The enzymatic phosphorylation of proteins. *J. Biol. Chem.* 211, 969–980
13 Fischer, E.H. and Krebs, E.G. (1955) Conversion of phosphorylase b to phosphorylase a in muscle extracts. *J. Biol. Chem.* 216, 121–132
14 Krebs, E.G. and Fischer, E.H. (1956) The phosphorylase b to a converting enzyme of rabbit skeletal muscle. *Biochim. Biophys. Acta* 20, 150–157
15 Walsh, D.A. *et al.* (1968) An adenosine 3′,5′-monophosphate-dependant protein kinase from rabbit skeletal muscle. *J. Biol. Chem.* 243, 3763–3765
16 Cohen, P. (2002) The origins of protein phosphorylation. *Nat. Cell Biol.* 4, E127–E130
17 Steelman, L.S. *et al.* (2004) JAK/STAT, Raf/MEK/ERK, PI3K/Akt and BCR-ABL in cell cycle progression and leukemogenesis. *Leukemia* 18, 189–218
18 The UniProt Consortium (2013) Update on activities at the Universal Protein Resource (UniProt) in 2013. *Nucleic Acids Res.* 41, D43–D47
19 Manning, G. *et al.* (2002) The protein kinase complement of the human genome. *Science* 298, 1912–1934
20 Pennisi, E. (2012) ENCODE project writes eulogy for junk DNA. *Science* 337, 1159–1161
21 Knighton, D. *et al.* (1991) Crystal structure of the catalytic subunit of cyclic adenosine monophosphate-dependent protein kinase. *Science* 253, 407–414
22 Tong, M. and Seeliger, M.A. (2015) Targeting conformational plasticity of protein kinases. *ACS Chem. Biol.* 10, 190–200
23 Noble, M.E.M. *et al.* (2004) Protein kinase inhibitors: insights into drug design from structure. *Science* 303, 1800–1805
24 Norman, R.A. *et al.* (2012) Structural approaches to obtain kinase selectivity. *Trends Pharmacol. Sci.* 33, 273–278
25 Cox, K.J. *et al.* (2010) Tinkering outside the kinase ATP box: allosteric (type IV) and bivalent (type V) inhibitors of protein kinases. *Future Med. Chem.* 3, 29–43
26 Lamba, V. and Ghosh, I. (2012) New directions in targeting protein kinases: focusing upon true allosteric and bivalent inhibitors. *Curr. Pharm. Des.* 18, 2936–2945
27 Yaish, P. *et al.* (1988) Blocking of EGF-dependent cell proliferation by EGF receptor kinase inhibitors. *Science* 242, 933–935
28 Gazit, A. *et al.* (1989) Tyrphostins I: synthesis and biological activity of protein tyrosine kinase inhibitors. *J. Med. Chem.* 32, 2344–2352
29 Gavrin, L.K. and Saiah, E. (2013) Approaches to discover non-ATP site kinase inhibitors. *MedChemComm* 4, 41–51
30 Wang, Q. *et al.* (2014) A structural atlas of kinases inhibited by clinically approved drugs. *Methods Enzymol.* 548, 23–67
31 Levitzki, A. (2013) Tyrosine kinase inhibitors: views of selectivity, sensitivity, and clinical performance. *Annu. Rev. Pharmacol. Toxicol.* 53, 161–185
32 Druker, B.J. *et al.* (2001) Efficacy and safety of a specific inhibitor of the BCR-ABL tyrosine kinase in chronic myeloid leukemia. *N. Eng. J. Med.* 344, 1031–1037
33 Panjarian, S. *et al.* (2013) Structure and dynamic regulation of Abl kinases. *J. Biol. Chem.* 288, 5443–5450
34 Winter, G.E. *et al.* (2012) Systems-pharmacology dissection of a drug synergy in imatinib-resistant CML. *Nat. Chem. Biol.* 8, 905–912
35 Nagar, B. *et al.* (2002) Crystal structures of the kinase domain of c-Abl in complex with the small molecule inhibitors PD173955 and imatinib (STI-571). *Cancer Res.* 62, 4236–4243
36 Lamontanara, A.J. *et al.* (2013) Mechanisms of resistance to BCR-ABL and other kinase inhibitors. *Biochim. Biophys. Acta* 1834, 1449–1459
37 Ma, L. *et al.* (2014) A therapeutically targetable mechanism of BCR-ABL-independent imatinib resistance in chronic myeloid leukemia. *Sci. Transl. Med.* 6, 252ra121
38 Levinson, N.M. and Boxer, S.G. (2014) A conserved water-mediated hydrogen bond network defines bosutinib's kinase selectivity. *Nat. Chem. Biol.* 10, 127–132
39 Xuan, Y-T. *et al.* (2001) An essential role of the JAK–STAT pathway in ischemic preconditioning. *Proc. Natl. Acad. Sci. U.S.A.* 98, 9050–9055
40 Meyer, S.C. and Levine, R.L. (2014) Molecular pathways: molecular basis for sensitivity and resistance to JAK kinase inhibitors. *Clin. Cancer Res.* 20, 2051–2059
41 Divito, S.J. and Kupper, T.S. (2014) Inhibiting Janus kinases to treat alopecia areata. *Nat. Med.* 20, 989–990
42 Doles, J.D. and Olwin, B.B. (2014) The impact of JAK–STAT signaling on muscle regeneration. *Nat. Med.* 20, 1094–1095
43 Geyer, H.L. and Mesa, R.A. (2014) Therapy for myeloproliferative neoplasms: when, which agent, and how? *Blood* 124, 3529–3537
44 Chrencik, J.E. *et al.* (2010) Structural and thermodynamic characterization of the TYK2 and JAK3 kinase domains in complex with CP-690550 and CMP-6. *J. Mol. Biol.* 400, 413–433
45 Williams, N.K. *et al.* (2009) Dissecting specificity in the Janus kinases: the structures of JAK-specific inhibitors complexed to the JAK1 and JAK2 protein tyrosine kinase domains. *J. Mol. Biol.* 387, 219–232
46 Goedken, E.R. *et al.* (2014) Tricyclic covalent inhibitors selectively target Jak3 through an active-site thiol. *J. Biol. Chem.* 298, 4573–4589
47 Gehringer, M. *et al.* (2014) Novel hinge-binding motifs for Janus kinase 3 inhibitors: a comprehensive structure–activity relationship study on tofacitinib bioisosteres. *ChemMedChem* 9, 2516–2527
48 Hynes, N.E. and Lane, H.A. (2005) ERBB receptors and cancer: the complexity of targeted inhibitors. *Nat. Rev. Cancer* 5, 341–354
49 Littlefield, P. *et al.* (2014) Structural analysis of the EGFR/HER3 heterodimer reveals the molecular basis for activating HER3 mutations. *Sci. Signal.* 7, ra114
50 Citri, A. and Yarden, Y. (2006) EGF–ERBB signalling: towards the systems level. *Nat. Rev. Mol. Cell Biol.* 7, 505–516
51 Yun, C-H. *et al.* (2007) Structures of lung cancer-derived EGFR mutants and inhibitor complexes: mechanism of activation and insights into differential inhibitor sensitivity. *Cancer Cell* 11, 217–227
52 Gajiwala, K.S. *et al.* (2013) Insights into the aberrant activity of mutant EGFR kinase domain and drug recognition. *Structure* 21, 209–219
53 Stamos, J. *et al.* (2002) Structure of the epidermal growth factor receptor kinase domain alone and in complex with a 4-anilinoquinazoline inhibitor (erlotinib with EGFR). *J. Biol. Chem.* 277, 46265–46272
54 Wood, E.R. *et al.* (2004) A unique structure for epidermal growth factor receptor bound to GW572016 (lapatinib): relationships among protein conformation, inhibitor off-rate, and receptor activity in tumor cells. *Cancer Res.* 64, 6652–6659
55 Qiu, C. *et al.* (2008) Mechanism of activation and inhibition of the HER4/ErbB4 kinase. *Structure* 16, 460–467
56 Fang, Z. *et al.* (2013) Strategies for the selective regulation of kinases with allosteric modulators: exploiting exclusive structural features. *ACS Chem. Biol.* 8, 58–70
57 Zhao, Z. *et al.* (2014) Exploration of type II binding mode: a privileged approach for kinase inhibitor focused drug discovery? *ACS Chem. Biol.* 9, 1230–1241
58 Knowles, P.P. *et al.* (2006) Structure and chemical inhibition of the RET tyrosine kinase domain. *J. Biol. Chem.* 281, 33577–33587
59 Ferrara, N. *et al.* (2003) The biology of VEGF and its receptors. *Nat. Med.* 9, 669–676
60 Olofsson, B. *et al.* (1996) Vascular endothelial growth factor B, a novel growth factor for endothelial cells. *Proc. Natl. Acad. Sci. U.S.A.* 93, 2576–2581
61 McTigue, M. *et al.* (2012) Molecular conformations, interactions, and properties associated with drug efficiency and clinical performance among VEGFR TK inhibitors. *Proc. Natl. Acad. Sci. U.S.A.* 109, 18281–18289
62 Simard, J.R. *et al.* (2009) Development of a fluorescent-tagged kinase assay system for the detection and characterization of allosteric kinase inhibitors. *J. Am. Chem. Soc.* 131, 13286–13296
63 Harris, P.A. *et al.* (2008) Discovery of 5-[[4-[(2,3-dimethyl-2H-indazol-6-yl)methylamino]-2-pyrimidinyl]amino]-2-methyl-benzenesulfonamide (pazopanib), a novel and potent vascular endothelial growth factor receptor inhibitor. *J. Med. Chem.* 51, 4632–4640
64 Okamoto, K. *et al.* (2015) Distinct binding mode of multikinase inhibitor lenvatinib revealed by biochemical characterization. *ACS Med. Chem. Lett.* 6, 89–94
65 Chiarle, R. *et al.* (2008) The anaplastic lymphoma kinase in the pathogenesis of cancer. *Nat. Rev. Cancer* 8, 11–23
66 Awad, M.M. and Shaw, A.T. (2014) ALK inhibitors in non-small cell lung cancer: crizotinib and beyond. *Clin. Adv. Hematol. Oncol.* 12, 429–439

67 Awad, M.M. *et al.* (2013) Acquired resistance to crizotinib from a mutation in CD74–ROS1. *N. Eng. J. Med.* 368, 2395–2401
68 Cui, J.J. *et al.* (2011) Structure based drug design of crizotinib (PF-02341066), a potent and selective dual inhibitor of mesenchymal–epithelial transition factor (c-MET) kinase and anaplastic lymphoma kinase (ALK). *J. Med. Chem.* 54, 6342–6363
69 Shaw, A.T. *et al.* (2014) Ceritinib in ALK-rearranged non-small-cell lung cancer. *N. Eng. J. Med.* 370, 1189–1197
70 Friboulet, L. *et al.* (2014) The ALK inhibitor ceritinib overcomes crizotinib resistance in non-small cell lung cancer. *Cancer Discov.* 4, 662–673
71 Stamos, J. *et al.* (2004) Crystal structure of the HGF β-chain in complex with the Sema domain of the Met receptor. *EMBO J.* 23, 2325–2335
72 Basilico, C. *et al.* (2008) A high affinity hepatocyte growth factor-binding site in the immunoglobulin-like region of Met. *J. Biol. Chem.* 283, 21267–21277
73 Trusolino, L. *et al.* (2010) MET signalling: principles and functions in development, organ regeneration and cancer. *Nat. Rev. Mol. Cell Biol.* 11, 834–848
74 Gelsomino, F. *et al.* (2014) MET and small-cell lung cancer. *Cancers* 6, 2100–2115
75 Katayama, R. *et al.* (2015) Cabozantinib overcomes crizotinib resistance in ROS1 fusion positive cancer. *Clin. Cancer Res.* 21, 166–174
76 Solca, F. *et al.* (2012) Target binding properties and cellular activity of afatinib (BIBW 2992), an irreversible ErbB family blocker. *J. Pharmacol. Exp. Ther.* 343, 342–350
77 Hendriks, R.W. *et al.* (2014) Targeting Bruton's tyrosine kinase in B cell malignancies. *Nat. Rev. Cancer* 14, 219–232
78 Byrd, J.C. *et al.* (2013) Targeting BTK with ibrutinib in relapsed chronic lymphocytic leukemia. *N. Eng. J. Med.* 369, 32–42
79 Garber, K. (2014) Kinase inhibitors overachieve in CLL. *Nat. Rev. Drug Discov.* 13, 162–164
80 Marcotte, D.J. *et al.* (2010) Structures of human Bruton's tyrosine kinase in active and inactive conformations suggest a mechanism of activation for TEC family kinases. *Protein Sci.* 19, 429–439
81 Bollag, G. *et al.* (2012) Vemurafenib: the first drug approved for BRAF-mutant cancer. *Nat. Rev. Drug Discov.* 11, 873–886
82 Wan, P.T.C. *et al.* (2004) Mechanism of activation of the RAF–ERK signaling pathway by oncogenic mutations of B-RAF. *Cell* 116, 855–867
83 Bollag, G. *et al.* (2010) Clinical efficacy of a RAF inhibitor needs broad target blockade in BRAF-mutant melanoma. *Nature* 467, 596–599
84 Pulici, M. *et al.* (2014) Optimization of diarylthiazole B-Raf inhibitors: identification of a compound endowed with high oral antitumor activity, mitigated hERG inhibition, and low paradoxical effect. *ChemMedChem* 10, 276–295
85 Luke, J.J. *et al.* (2014) The biology and clinical development of MEK inhibitors for cancer. *Drugs* 74, 2111–2128
86 Abe, H. *et al.* (2011) Discovery of a highly potent and selective MEK inhibitor: GSK1120212 (JTP-74057 DMSO solvate). *ACS Med. Chem. Lett.* 2, 320–324
87 Dong, Q. *et al.* (2011) Discovery of TAK-733, a potent and selective MEK allosteric site inhibitor for the treatment of cancer. *Bioorg. Med. Chem. Lett.* 21, 1315–1319
88 Flaherty, K.T. *et al.* (2012) Combined BRAF and MEK inhibition in melanoma with BRAF V600 mutations. *N. Eng. J. Med.* 367, 1694–1703
89 Long, G.V. *et al.* (2014) Combined BRAF and MEK inhibition versus BRAF inhibition alone in melanoma. *N. Eng. J. Med.* 371, 1877–1888
90 Wu, P. and Hu, Y.Z. (2010) PI3K/Akt/mTOR pathway inhibitors in cancer: a perspective on clinical progress. *Curr. Med. Chem.* 17, 4326–4341
91 Chiarini, F. *et al.* (2015) Current treatment strategies for inhibiting mTOR in cancer. *Trends Pharmacol. Sci.* 36, 124–135
92 Choi, Y.J. and Anders, L. (2014) Signaling through cyclin D-dependent kinases. *Oncogene* 33, 1890–1903
93 Casimiro, M.C. *et al.* (2014) Overview of cyclins D1 function in cancer and the CDK inhibitor landscape: past and present. *Expert Opin. Investig. Drugs* 23, 295–304
94 Lu, H. and Schulze-Gahmen, U. (2006) Toward understanding the structural basis of cyclin-dependent kinase 6 specific inhibition. *J. Med. Chem.* 49, 3826–3831
95 Whitman, M. *et al.* (1985) Association of phosphatidylinositol kinase activity with polyoma middle-T competent for transformation. *Nature* 315, 239–242
96 Wu, P. *et al.* (2009) PI3K inhibitors for cancer therapy: what has been achieved so far? *Curr. Med. Chem.* 16, 916–930
97 Furman, R.R. *et al.* (2014) Idelalisib and rituximab in relapsed chronic lymphocytic leukemia. *N. Eng. J. Med.* 370, 997–1007
98 Cheson, B.D. (2014) CLL and NHL: the end of chemotherapy? *Blood* 123, 3368–3370
99 Ali, K. *et al.* (2014) Inactivation of PI_3K p110δ breaks regulatory T-cell-mediated immune tolerance to cancer. *Nature* 510, 407–411
100 Berndt, A. *et al.* (2010) The p110δ structure: mechanisms for selectivity and potency of new PI_3K inhibitors. *Nat. Chem. Biol.* 6, 117–124
101 Somoza, J.R. *et al.* (2015) Structural, biochemical and biophysical characterization of idelalisib binding to phosphoinositide 3-kinase δ. *J. Biol. Chem.* 290, 8439–8446
102 Wu, P. and Hu, Y. (2012) Small molecules targeting phosphoinositide 3-kinases. *MedChemComm* 3, 1337–1355
103 Flinn, I.W. *et al.* (2014) Idelalisib, a selective inhibitor of phosphatidylinositol 3-kinase-δ, as therapy for previously treated indolent non-Hodgkin lymphoma. *Blood* 123, 3406–3413
104 Brown, J.R. *et al.* (2014) Idelalisib, an inhibitor of phosphatidylinositol 3-kinase p110δ, for relapsed/refractory chronic lymphocytic leukemia. *Blood* 123, 3390–3397
105 Fruman, D.A. and Rommel, C. (2014) PI3K and cancer: lessons, challenges and opportunities. *Nat. Rev. Drug Discov.* 13, 140–156
106 Costa, C. *et al.* (2015) Measurement of PIP3 levels reveals an unexpected role for p110β in early adaptive responses to p110α-specific inhibitors in luminal breast cancer. *Cancer Cell* 27, 97–108
107 Schwartz, S. *et al.* (2015) Feedback suppression of PI3Kα signaling in PTEN-mutated tumors is relieved by selective inhibition of PI3Kβ. *Cancer Cell* 27, 109–122
108 Kinch, M.S. (2014) An analysis of FDA-approved drugs for oncology. *Drug Discov. Today* 19, 1831–1835
109 Davis, M.I. *et al.* (2011) Comprehensive analysis of kinase inhibitor selectivity. *Nat. Biotechnol.* 29, 1046–1051
110 Rask-Andersen, M. *et al.* (2014) The druggable genome: evaluation of drug targets in clinical trials suggests major shifts in molecular class and indication. *Annu. Rev. Pharmacol. Toxicol.* 54, 9–26